REPORT SERIES IN AEROSOL SCIENCE
N:o 167 (2015)

NANOPARTICLE VOLATILITY AND GROWTH:

Implications for interactions between biogenic and anthropogenic aerosol components

SILJA HÄME (NÉE HÄKKINEN)

Division of Atmospheric Sciences
Department of Physics
Faculty of Science
University of Helsinki
Helsinki, Finland

Academic dissertation

To be presented, with the permission of the Faculty of Science of the University of Helsinki, for public criticism in auditorium E204, Gustaf Hällströmin katu 2, on May 28th, 2015, at 12 o'clock noon.

Helsinki 2015

Author's Address: Department of Physics
P.O. Box 64
FI-00014 University of Helsinki
silja.hakkinen@helsinki.fi

Supervisors: Docent Ilona Riipinen, Ph.D.
Department of Physics
University of Helsinki /
Department of Analytical Chemistry and Environmental Science
Stockholm University

Professor Tuukka Petäjä, Ph.D.
Department of Physics
University of Helsinki

Professor V. Faye McNeill, Ph.D.
Department of Chemical Engineering
Columbia University in the city of New York

Reviewers: Associate Professor Joel Thornton, Ph.D.
Department of Atmospheric Sciences
University of Washington

Associate Professor Miikka Dal Maso, Ph.D.
Department of Physics
Tampere University of Technology

Opponent: Professor Astrid Kiendler-Scharr, Ph.D.
Institut für Energie und Klimaforschung, IEK-8
Forschungszentrum Jülich

ISBN 978-952-7091-22-7 (printed version)
ISSN 0784-3496
Helsinki 2015
Unigrafia Oy

ISBN 978-952-7091-23-4 (pdf version)
http://ethesis.helsinki.fi
Helsinki 2015
Helsingin yliopiston verkkojulkaisut

Acknowledgements

The research for this thesis was carried out at the University of Helsinki, Department of Physics, Division of Atmospheric Sciences. I thank the present head of the department Prof. Hannu Koskinen and his predecessor Prof. Juhani Keinonen for providing me with the working facilities. I express my gratitude to the head of the division Prof. Markku Kulmala for providing me a great opportunity to work in one of the most renowned research groups in the field of atmospheric sciences.

I thank my supervisor Prof. Ilona Riipinen for the dedicated guidance she has provided me throughout the years. Her enthusiasm, vision, patience and support have been invaluable. Ilona has always encouraged me to go a little bit further and I owe much of this thesis to her. I want to thank Prof. Tuukka Petäjä for his guidance. His expertise in the field of atmospheric measurements and instrumentation has been of great importance during my research work. I owe special thanks to Prof. Faye McNeill who warmly welcomed me to join her group at Columbia University in the city of New York for two years, 2012-2014. Her supervision, encouragement and feedback during those years was valuable. She provided me not only with the laboratory facilities to work on my own project but also the opportunity to collaborate with research groups at Rutgers University and Georgia Institute of Technology.

I thank Prof. Miikka Dal Maso and Prof. Joel Thornton for reviewing this thesis.

I want to acknowledge all my co-authors for their contribution to the research work presented in this thesis. I thank M.Sc. Mikko Äijälä for useful discussions especially concerning aerosol mass spectrometry. I thank Dr. Alison Schwier and Dr. Joe Woo for helping me to learn my way around the lab. I wish to thank all my co-workers at the Division of Atmospheric Sciences for making the working environment pleasant and inspiring. I thank the McNeill group for the years we spend together – both science- and fun-related.

This thesis has been financially supported by Finnish Academy of Science and Letters which is gratefully acknowledged. The visit to Columbia University was made possible by Finnish Fulbright Commission who provided funding and support during my stay in New York, which I greatly appreciate.

I want to thank my physicist friends who I have shared the academic path with for friendship and understanding the perks (and cons) of being a scientist. I want to thank my friends outside the academia for reminding me that there is more to life than science. I want to thank my parents and sisters for their love and support. Finally, I wish to thank my husband Yrjö for his love and encouragement. Because of him, I got off my comfort zone, moved to the U.S. and had the time of my life while doing a PhD.

Silja Alma Kaarina Häme (née Häkkinen)

University of Helsinki, 2015

Abstract

Aerosol particles are important atmospheric constituents. They exist in both polluted and remote areas but the sizes and concentrations of these particles vary greatly depending on location. Aerosol particles damage human health via inhalation, reduce visibility with high mass loadings, and among all, contribute to climate change. Particles directly scatter and absorb solar radiation. In addition, particles that are large enough can participate in cloud formation and affect cloud properties by acting as cloud condensation nuclei (CCN).

A notable fraction of submicron atmospheric aerosol mass consists of organic compounds, and a large fraction of this material has been formed through condensation of organic vapors onto aerosol particles (secondary organic aerosol, SOA). Most of the global SOA mass is deemed to be biogenic in origin, but recent studies suggest that a significant fraction of it may be controlled by anthropogenic pollution. However, due to poor understanding of this anthropogenic enhancement in biogenic SOA formation, it is not systematically accounted for in current atmospheric models. Due to these kind of uncertainties in global SOA mass burden and lack of detailed knowledge of chemical, physical and optical properties of SOA, estimates of organic aerosol effect on the climate are highly uncertain.

To decrease the uncertainty in the climate effects of the organic aerosol, an improved understanding of the formation mechanisms and properties of SOA is needed. In addition, nanoparticle growth to CCN-sizes by condensation of secondary organic matter needs to be accurately described in atmospheric models. In this thesis the formation of SOA is investigated in the presence of both biogenic and anthropogenic compounds. The chemical and physical properties – volatility and hygroscopicity – of SOA are examined via field and laboratory experiments combined with process modeling. The thesis introduces improvements for the treatment of SOA related to nanoparticle growth in atmospheric models and evaluates their performance.

The thesis shows that interactions between atmospheric biogenic and anthropogenic aerosol components can form aerosol material of low-volatility. For instance organic salt formation via chemical reactions between organic acids and inorganic salts can lower aerosol volatility. Particulate-phase processing may also alter aerosol hygroscopic properties. Description of nanoparticle growth by low-volatility secondary organics is important in improving the estimates of particle and CCN numbers. The thesis highlights the significance of biogenic organic matter formed under anthropogenic influence in the nanoparticle growth. This warrants future studies focusing on the formation mechanisms and properties of anthropogenically driven biogenic organic aerosol.

Keywords: secondary organic aerosol, anthropogenic influence, particulate-phase processing, volatility, condensational growth, CCN

Contents

1 Introduction 7
2 Definitions and theoretical background 11
2.1 Low-volatility aerosol constituents 12
2.2 Aerosol condensational growth and evaporation 13
3 Experimental methods and data analysis 16
3.1 Volatility measurements 16
3.1.1 VDMPS for particle-phase measurements 17
3.1.2 TPD aerosol-CIMS for gaseous-phase measurements 18
3.2 Quantitative assessment of the volatility of aerosol constituents from measurements 20
3.2.1 Methods based on experimental data 20
3.2.2 Methods coupling experimental data with mass-transfer model 20
3.3 Experimental data used for nanoparticle growth parameterization 23
4 Results and discussion 24
4.1 Volatility of boreal forest aerosol 24
4.2 Volatility of organic acid - inorganic salt aerosol mixtures 27
4.2.1 Evaluating TPD aerosol-CIMS performance with pure organic acids 27
4.2.2 Organic salt formation 27
4.2.3 Discussion on volatility of organic salts 29
4.2.4 Discussion on hygroscopicity of organic salts 31
4.3 Semi-empirical size-dependent parameterization for nanoparticle growth 31
5 Review of papers and the author's contribution 38
6 Conclusions 40
References 44

List of publications

This thesis consists of an introductory review, followed by 5 research articles. In the introductory part, the papers are cited according to their roman numerals.

I Häkkinen, S. A. K., Äijälä, M., Lehtipalo, K., Junninen, H., Backman, J., Virkkula, A., Nieminen, T., Vestenius, M., Hakola, H., Ehn, M., Worsnop, D. R., Kulmala, M., Petäjä, T., and Riipinen, I. (2012). Long-term volatility measurements of submicron atmospheric aerosol in Hyytiälä, Finland. *Atmos. Chem. Phys.*, 12(22): 10771-10786. Reproduced under Creative Commons Attribution License.

II Häkkinen, S. A. K., McNeill, V. F., and Riipinen, I. (2014). Effect of inorganic salts on the volatility of organic acids. *Environ. Sci. Technol.*, 48(23): 13718-13726, DOI: 10.1021/es5033103. Copyright 2014 American Chemical Society. Reproduced with permission.

III Drozd, G., Woo, J., Häkkinen, S. A. K., Nenes, A., and McNeill, V. F. (2014). Inorganic salts interact with oxalic acid in submicron particles to form material with low hygroscopicity and volatility. *Atmos. Chem. Phys.*, 14(10): 5205-5215. Reproduced under Creative Commons Attribution License.

IV Häkkinen, S. A. K., Manninen, H. E., Yli-Juuti, T., Merikanto, J., Kajos, M. K., Nieminen, T., D'Andrea, S. D., Asmi, A., Pierce, J. R., Kulmala, M., and Riipinen, I. (2013). Semi-empirical parameterization of size-dependent atmospheric nanoparticle growth in continental environments. *Atmos. Chem. Phys.*, 13(15): 7665-7682. Reproduced under Creative Commons Attribution License.

V D'Andrea, S. D., Häkkinen, S. A. K., Westervelt, D. M., Kuang, C., Levin, E. J. T., Kanawade, V. P., Leaitch, W. R., Spracklen, D. V., Riipinen, I., and Pierce, J. R. (2013). Understanding global secondary organic aerosol amount and size-resolved condensational behavior. *Atmos. Chem. Phys.*, 13(22): 11519-11534. Reproduced under Creative Commons Attribution License.

1 Introduction

The Earth's atmosphere consists of a mixture of gases and small liquid or solid particles. Both the sizes and concentrations of these aerosol particles vary depending on location. Particles can be as small as large molecules (~ 1 nm in diameter) or so big that human eye is able to distinguish a single particle (~ 0.1 mm). In urban polluted environments particle number concentrations can exceed 1 000 000 cm^{-3} while in remote clean areas number concentrations are often 10-100 cm^{-3} (Seinfeld and Pandis, 2006). Similarly, in polluted cities, daily average mass concentrations of submicron particles can reach 400 µg m^{-3}, whereas in remote regions the monitored values are on average below 10 µg m^{-3} (Zhang et al., 2007; Jimenez et al., 2009; Huang et al., 2014).

High loadings of atmospheric submicron particles can deteriorate visibility (Cabada et al., 2004) and cause adverse acute and chronic health effects via inhalation of air (Dockery et al., 1993; Davidson et al., 2005; Nel, 2005; Mauderly and Chow, 2008). Aerosol particles also affect regional and global climate (IPCC, 2013). They influence the Earth's radiative balance by affecting the fraction of the incoming solar radiation that is radiated back to space. Depending on aerosol chemical composition, particles can either directly scatter (e.g. sulfate) or absorb (e.g. soot) solar radiation (Schulz et al., 2006; Stier et al., 2007). In addition, particles that are large enough – roughly 50 nm in dry diameter or larger – can act as seeds for cloud droplets (cloud condensation nuclei, CCN, Dusek et al., 2006; Kerminen et al., 2012). Clouds, in turn, can reflect solar radiation back to space and cool the climate. Aerosol particles thus indirectly affect the climate by modifying cloud properties and lifetime (Ramanathan et al., 2001; Lohmann and Feichter, 2005).

Aerosol particles consist of both inorganic and organic species. Volatility is the main property of an atmospheric compound determining how large fraction of it stays in the particle-phase under ambient conditions. The lower the volatility of a compound is, the larger this fraction is. While the sources, chemistry and properties of aerosol inorganic compounds are relatively well-known, less is known about atmospheric organics. Thousands of organic compounds are present in both gaseous and particulate phases, and a large fraction of them remain unidentified (Goldstein and Galbally, 2007). Organic compounds contribute significantly to particle chemical composition: 20-90% of the total submicron aerosol mass consists of organics depending on location (Kanakidou et al., 2005; Zhang et al., 2007; Jimenez et al., 2009).

Organic aerosol (OA) consists of primary and secondary organics. Primary organic aerosol (POA) is directly emitted from both anthropogenic and biogenic sources, while secondary organic aerosol (SOA) is formed upon gas-to-particle conversion from condensable vapors. The dominant fraction of submicron organic aerosol is estimated to be secondary (Zhang et al., 2007; Hallquist et al., 2009; Jimenez et al., 2009). While most of the global secondary organic aerosol is expected to be biogenic (BSOA), anthropogenic precursors can be an equally important source of secondary organic aerosol mass (e.g. fossil fuel SOA, FSOA) in urban regions of northern mid-latitudes (De Gouw and Jimenez, 2009). Recently,

enhanced formation of secondary organic aerosol from biogenic precursors in the presence of anthropogenic pollutants (eBSOA) has drawn attention suggesting that strict separation of atmospheric SOA to its natural and anthropogenic components solely based on the origin of the precursor may not be possible (Fig. 1) (Weber et al., 2007; Carlton et al., 2010; Hoyle et al., 2011; Spracklen et al., 2011). In the Eastern United States, anthropogenic pollution is likely to explain around half or even more of the present-day biogenic secondary organic aerosol mass (Carlton et al., 2010; Carlton and Turpin, 2013).

Estimates of total organic aerosol mass budgets – especially for SOA – are highly uncertain due to poorly constrained sources and sinks of organic aerosol, as well as the relative contributions of these to organic aerosol mass. Estimates of global SOA source range from 20 to 380 Tg year^{-1} (Hallquist et al., 2009; Heald et al., 2011; Spracklen et al., 2011).

Currently, many large-scale atmospheric models account for "traditional" SOA – secondary organic matter formed from natural precursors (monoterpenes and isoprene) via atmospheric oxidation – while some of them take into account also "non-traditional" SOA from aqueous-phase oxidation of organics (Tsigaridis et al., 2014). Very few models account for SOA from anthropogenic precursors even though its contribution is not insignificant (Volkamer et al., 2006; Farina et al., 2010; Myhre et al., 2013; Tsigaridis et al., 2014). In addition, anthropogenically enhanced biogenic SOA is not systematically accounted for in global climate or chemistry models although indications of its importance exist (Spracklen et al., 2011; Tsigaridis et al., 2014).

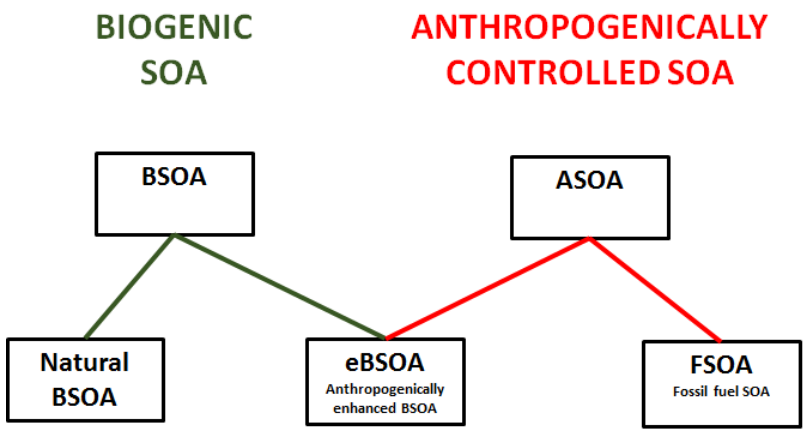

Figure 1: Definitions of secondary organic aerosol (SOA) forming from natural or anthropogenic precursors and in the presence of both natural compounds and anthropogenic pollutants used in this work. Natural BSOA includes both "traditional" and "non-traditional" secondary organics. Definitions are adapted from Hoyle et al. (2011) and Tsigaridis et al. (2014).

Besides affecting the overall mass burden of atmospheric particulate matter, organic compounds influence CCN numbers by growing freshly formed nanoparticles to larger sizes. Growth of the smallest particles by condensation of low-volatility secondary organic matter is a significant source of CCN – linking nanoparticle growth to secondary organic aerosol formation (Merikanto et al., 2009; Riipinen et al., 2011). Uncertainties in CCN numbers and properties are rising from both uncertainties in the total SOA burden (Good et al., 2010) as well as inconsistent treatment of SOA related to nanoparticle growth in large-scale models (Pierce et al., 2011; Riipinen et al., 2011). It is known that low-volatility secondary organic compounds can be formed in both the gaseous and particulate phase via interactions of aerosol constituents, e.g. in organic-inorganic aerosol. (Kroll and Seinfeld, 2008; Riipinen et al., 2012; Ehn et al., 2014). However, the exact formation mechanisms, identities and properties of these compounds are not fully constrained.

Currently in atmospheric models, organic condensation onto pre-existing aerosol size distribution is typically done either proportional to total organic particle mass ("thermodynamic approach") or surface area ("kinetic approach") (see Riipinen et al., 2011). Both of these condensation schemes have their advantages and disadvantages – the thermodynamic approach captures particle mass loadings better but fails to represent size-dependent growth of ultrafine (< 100 nm) particles, whereas the kinetic approach captures the growth of the smallest particles better but does not account for the volatility and re-evaporation of the condensable organics. When estimating CCN concentrations, the kinetic approach is likely to perform better than the thermodynamic one since it enables nanoparticle growth to CCN sizes. An ideal model would include both of these schemes. However, complete modeling schemes are often computationally too time consuming to be applicable in large-scale models and thus simplified parameterizations of the condensation processes of secondary organics are needed.

According to the most recent report by the Intergovernmental Panel for Climate Change (IPCC, 2013), the anthropogenic aerosol net effect on climate is cooling: the industrial era effective radiative forcing is estimated to be around -0.9 W m^{-2}. This is opposite to the effect of greenhouse gases with an effective radiative forcing of 2.8 W m^{-2}. When the climate effects of anthropogenic aerosol are assessed component by component, the global climate impact of anthropogenic secondary organic aerosol (ASOA, Fig. 1) is estimated to be minimal with large uncertainties, with direct radiative forcing of -0.03 W m^{-2}, estimates ranging from -0.27 up to 0.20 W m^{-2} (IPCC, 2013).

However, recent studies suggest that the cooling effect of anthropogenic secondary organic aerosol may be underestimated in the IPCC models. For instance, Spracklen et al. (2011) estimated the direct radiative forcing of ASOA to be around -0.26 W m^{-2} when it is accounted for to the extent suggested by model-measurement comparisons – being in the lower end of the estimate by IPCC (2013). Hence, significant differences in the estimated radiative forcings of organic aerosol are expected with different amounts and formation mechanisms of anthropogenically controlled organic aerosol in the models (Spracklen et al., 2011; Myhre et al., 2013; Tsigaridis et al., 2014). Furthermore, estimation on the radiative forcing of anthropogenically controlled organic aerosol concerning cloud formation was not

provided in the IPCC (2013) report, even though it may notably contribute to the cooling of the climate by aerosols (Spracklen et al., 2011). To decrease the uncertainty in the climate effects of organic aerosol, more accurate descriptions of anthropogenically driven organic aerosol formation and properties, and its contribution to particle growth are warranted.

This thesis provides novel insights on the following research topics: gas-particle partitioning of organic matter and volatilities of aerosol constituents, particulate-phase chemical reactions, and nanoparticle growth by atmospheric secondary organics. The thesis seeks answers for the following research questions, with a special focus on the interactions between organic and inorganic as well as natural and anthropogenic atmospheric constituents:

1) Which compounds contribute to the extremely low-volatility matter in submicron aerosol particles? (Q1)

2) How does low-volatility aerosol material form in the particulate phase, and how does it modify aerosol properties? (Q2)

3) What is the significance of low-volatility secondary organics in the growth of nanoparticles (< 20 nm in diameter), and how should the growth be described in atmospheric models to estimate aerosol particle and CCN number concentrations? (Q3)

The research is performed by field and laboratory measurements as well as process modeling. **Paper I** focuses on Q1 with a long-term data set measured in a boreal forest environment in Hyytiälä, Finland, providing indirect input to also Q2 and Q3. Concerning Q2, organic-inorganic particles mimicking simple atmospheric aerosol are generated in laboratory conditions, and measurements on aerosol volatility are utilized to obtain information on particulate-phase processing in **Papers II and III**. **Paper II** further introduces a novel method for quantitative measurements of the volatilities of organic aerosol constituents, thus also contributing to Q1. Concerning Q3, physically-based semi-empirical parameterization capturing sub-20 nm particle growth by atmospheric condensable vapors is developed in **Paper IV**, and its performance is assessed in a global-scale atmospheric model in **Paper V**.

2 Definitions and theoretical background

The volatility of a compound describes the tendency of a molecule to escape from the particle surface. For pure components, volatility is quantified by saturation vapor pressure (p_{sat}) and vaporization enthalpy (ΔH_{vap}). p_{sat} is the partial pressure of a condensable vapor in a gas-liquid (or solid) equilibrium in which the rate of molecules entering a flat liquid (or solid) surface equals the rate at which molecules escape from the surface. For multicomponent systems and over curved surfaces, the equilibrium vapor pressure (p_{eq}) depends on the mixture composition, curvature and the pure-component p_{sat}s of the mixture constituents. ΔH_{vap} describes the temperature-dependency of p_{sat}.

Most freshly emitted atmospheric organic compounds are volatile, with C_{sat} of 10^7 µg m^{-3} or higher (Table 1). As an example, in boreal forest areas typical maximum concentrations of monoterpenes are around 10 µg m^{-3} (**Paper IV**). The volatile organic compounds (VOCs) can form compounds with lower volatilities through atmospheric oxidation, resulting in semivolatile organic compounds (SVOCs), low-volatility organic compounds (LVOCs) and extremely low-volatility organic compounds (ELVOCs) (Donahue et al., 2013, Murphy, 2014). Organic compounds can be categorized based on their pure-component saturation vapor pressures (or concentrations) (Table 1).

Table 1: Definitions related to organic compounds of different volatilities following Donahue et al. (2013) and Murphy et al. (2014). Saturation vapor pressures (p_{sat}), and mass (C_{sat}) and number concentrations (N_{sat}) in standard conditions are given. The exponents are given as integers for simplification (to be exact e.g. C_{sat} range of SVOC should be written as $10^{-0.5}$-$10^{2.5}$ µg m^{-3}).

Name	Abbreviation	p_{sat} (Pa)	C_{sat} (µg m^{-3})	$N_{sat,}$ (molec cm^{-3})
Volatile organic compounds	VOC	$\geq 10^2$	$\geq 10^7$	$\geq 5 \cdot 10^{16}$
Intermediate volatility organic compounds	IVOC	10^{-2}-10^1	10^3-10^6	$5 \cdot 10^{12}$-$5 \cdot 10^{15}$
Semivolatile organic compounds	SVOC	10^{-5}-10^{-3}	10^0-10^2	$5 \cdot 10^9$-$5 \cdot 10^{11}$
Low-volatility organic compounds	LVOC	10^{-8}-10^{-6}	10^{-3}-10^{-1}	$5 \cdot 10^6$-$5 \cdot 10^8$
Extremely low-volatility organic compounds	ELVOC	$\leq 10^{-9}$	$\leq 10^{-4}$	$\leq 5 \cdot 10^5$

Terms “non-volatile” or “effectively non-volatile” are not well defined even though they are widely used. This is because the volatility depends on ambient conditions such as temperature. In this thesis “non-volatile” is used to describe aerosol matter that is not evaporated after spending approximately 1 s at temperatures around 160 ˚C and above. Hence, the used terminology is, in this context related to the instrumental abilities (**Papers I-III**). In this thesis, “non-volatile” aerosol material can be associated with low-volatility and extremely low-volatility matter (Table 1).

2.1 Low-volatility aerosol constituents

Oxidized organic compounds of different volatilities will contribute to particle chemical composition depending on particle size. Ehn et al. (2014) reported gas-phase production of high-molecular mass ELVOCs upon oxidation of monoterpenes which can significantly contribute to nanoparticle (< 20 nm) growth. Organic material of low-volatility and extremely low-volatility can be also formed within the particle phase. This enhances organic aerosol formation by shifting the gas-particle equilibrium and thus enhancing gas-phase uptake of organics. Possible pathways for the formation of low-volatility matter in the aerosol are e.g. acid-base neutralizations reactions leading to organic salt formation, formation of organosulfates (sulfate esters) in the presence of acidified sulfate seed aerosol, and formation of high molecular-weight polymers from organic monomers (Riipinen et al., 2012).

Aminium salts formed within reactions between amines and carboxylic acids have been shown to be of low-volatility (p_{sat} of 10^{-9}-10^{-6} Pa), and a notable contribution to nanoparticle growth has been reported (Smith et al., 2010; Lavi et al., 2015). Organic salt formation within weak carboxylic acid-sea salt particles due to chloride depletion from the aerosol surface (Laskin et al., 2012), and within carboxylic acid-ammonium aerosol mixtures have also been reported (Dinar et al., 2008; Ortiz-Montalvo et al., 2014). Organic polymerization has been observed to occur both via acid-catalyzed reactions (Jang et al., 2002; Liggio et al., 2005; Surratt et al., 2007) and without an acidified seed aerosol (Gao et al., 2004; Kalberer et al., 2004). Acid-catalyzed reactions and other particle-phase reactions taking place under anthropogenic influence should be considered as possible contributors to eBSOA.

Concerning inorganic aerosol species, ammonium sulfate can be considered to be of extremely low-volatility while ammonium nitrate and sulfuric acid are semivolatile or of low-volatility: submicron ammonium sulfate aerosol evaporates at around 200 ˚C, sulfuric acid aerosol at around 100 ˚C and ammonium nitrate at around 50-75 ˚C given enough time for the evaporation to occur (e.g. O'Dowd et al., 1997; Johnson et al., 2004; An et al., 2007; Villani et al., 2007; Huffman et al., 2008; Tritscher et al., 2011). Submicron aerosol particles typically contain also refractory compounds such as soot (defined here as black carbon, BC) and sea salt, larger particles also crustal material. These compounds will not be evaporated in the typical aerosol heating units (discussed in Sect. 3.1) with maximum heating temperatures of around 300 ˚C. Most of atmospheric aerosol non-refractory inorganic and

organic constituents are volatilized below this temperature (Philippin et al., 2004). However, there is indirect evidence of organic aerosol components in submicron, even in freshly formed particles, that are not volatilized upon heating at around 300 ˚C (**Paper I**; Wehner et al., 2005; Ehn et al., 2007; Villani et al., 2007; Backman et al., 2010).

In addition to the volatility of the organic compounds, also their hygroscopicities are of interest. Hygroscopicity describes the ability of a compound to uptake water and is essential aerosol property when determining CCN formation. Formation of low-volatility organic matter in the particulate-phase can strongly affect particle hygroscopicity, for example ammonium and aminium salt formation may enhance aerosol CCN activity (Dinar et al., 2008; Smith et al., 2010; Lavi et al., 2015). This topic is further discussed in Sect. 4.2.4 in the light of **Paper III**.

2.2 Aerosol condensational growth and evaporation

If aerosol particles are not in equilibrium with the gas phase surrounding them, diffusion mass transfer of vapors to/from the particles occurs. Whether the net mass transfer is towards aerosol particles or from the particles, i.e. whether particles grow or evaporate, depends on both the volatility and the concentrations of the condensable vapors. When particles are larger than the mean free path of the vapors, typically of 10-100 nm (Vehkamäki and Riipinen, 2012), they "see" the surrounding gas phase as a continuum. In the continuum regime mass transfer to and from particles of d_p in diameter is determined using the bulk properties of the system. The mass flux of compound i (kg s^{-1}) to/from a spherical particle can be written as

$$I_i(d_p) = \frac{2\pi d_p D_i M_i p}{RT} \ln\left(\frac{1-\frac{p_{i,a}}{p}}{1-\frac{p_i}{p}}\right) \approx \frac{2\pi d_p D_i M_i}{RT}(p_i - p_{i,a}), \quad (1)$$

where M_i (g mol^{-1}) and D_i (m^2 s^{-1}) are the molar mass and diffusion coefficient of the compound, p is ambient pressure, T (K) is temperature, R is ideal gas constant, and $p_{a,i}$ and p_i are the partial pressures of i at particle surface and far from the particle, respectively. The presented approximation can be made if $p_i << p$. This is discussed in more detail below. Partial pressure of compound i at the particle surface is equal to the equilibrium vapor pressure, $p_{eq,i}$:

$$p_{i,a}(T) = p_{eq,i}(T) = X_i \gamma_i p_{sat,i}(T) \exp\left(\frac{4 v_{m,i} \sigma}{RT d_p}\right), \quad (2)$$

where X_i is the molar fraction of compound i in the aerosol, γ_i is the activity coefficient of compound i (assumed unity in this work), $p_{sat,i}$ is the saturation vapor pressure of pure compound i over flat surface, and the exponential term is the Kelvin effect, where σ (N m^{-1}) is particle surface tension calculated as mole weighted average over all aerosol constituents, and $v_{m,i}$ (m^3 mol^{-1}) is a partial molar volume of i. Partial pressure of compound i far from the particle can be written as

$$p_i(T) = \frac{C_i RT}{M_i}, \quad (3)$$

where C_i (μg m^{-3}) is the gas phase concentration of compound *i*. In Eq. 1 the logarithmic pressure-term multiplied by the total pressure includes a description of Stefan flow that is always present when condensation or evaporation takes place. Stefan flow can be neglected when the partial vapor pressures of the condensing vapors are much smaller than the total ambient pressure, as is often the case in the atmosphere. Then, the pressure-term can be replaced by difference $p_i - p_{i,eq}$. This difference essentially determines the fate of the particles – with ambient concentration of condensing vapor *i* higher than the equilibrium concentration of the particles, condensation occurs, and vice versa.

When particles are notably smaller than the mean free path of the gas molecules, less than about 10 nm in diameter, approach used for continuum regime conditions is not valid and mass transport to and from the particles should be determined on a molecular basis, using kinetic gas theory. In the kinetic regime, mass flux of condensable vapor *i* can be written following Lehtinen and Kulmala (2003)

$$I_i(d_p) = \frac{\frac{3}{2}\pi(d_i+d_p)(D_i+D_p(d_p))\frac{\alpha_{m,i}}{Kn}M_i}{RT}(p_i - p_{eq,i}), \quad (4)$$

where d_i is the diameter of a vapor molecule, D_p is the diffusion coefficient of a particle with diameter d_p, α_m is the mass accommodation coefficient (assumed unity in this work, see Winkler et al., 2006; Julin et al., 2014) and Kn is the Knudsen number Kn (ratio of the mean free path of compound *i* and the sum of particle and vapor molecule radii). Accounting for the diffusional movement of particles as well as the diameter of the vapor molecules is important only when the size of the vapor molecule is comparable to that of the particle.

In the atmosphere particle diameter is very often comparable to the mean free path of the gas molecules. In this case neither of the above presented approaches work well and thus, semi-empirical modifications to the mass transfer equations are needed in this transition regime. Most often used correction factor is β_m(Kn, α_m) by Fuchs and Sutugin (1970) which is a function of Kn and $\alpha_{m,i}$. This factor can be multiplied with the mass flux of continuum regime (Eq. 1) or used to replace $\frac{3\alpha_{m,i}}{4Kn}$ -term in the kinetic regime mass flux (Eq. 4) to be able to capture mass transfer to and from transition regime particles.

When considering nanoparticle growth to larger sizes, diameter growth rate (GR, nm h^{-1}) is often determined from experimental data such as aerosol size distribution measurements (see Sect. 3.3 and Weber et al., 1997; Kulmala et al., 2004; Dal Maso et al., 2005; Hirsikko et al., 2005; Stolzenburg et al., 2005; Manninen et al., 2010; Yli-Juuti et al., 2011; Yu et al., 2014). If particle concentrations and thus coagulation rates are low enough (Kerminen and Kulmala, 2002), GR can be linked to the condensational mass flux as follows

$$I_{tot}(d_p) = \frac{1}{2}\pi\rho_p d_p^2 GR(d_p), \quad (5)$$

where I_{tot} is the total mass flux towards the particle population with diameter of d_p (Vehkamäki and Riipinen, 2012). With the basic mass transfer equations presented above, particle growth by each species (*i*) can be determined if the gas-phase concentrations of the condensing species and their p_{sat}s are known. In modeling approaches aiming to capture

nanoparticle growth, p_{sat} of the condensing compound is often set to zero and thus, p_{eq} becomes zero. In these kind of models, condensation is treated as irreversible and the mass transfer depends only on the ambient concentration of the condensing species (Spracklen et al., 2005a; Spracklen et al., 2005b; Pierce and Adams, 2009; Riipinen et al., 2011). For atmospheric vapors such as sulfuric acid and ELVOCs, this assumption is valid but since a large fraction of the condensable organic matter is semivolatile, growth of the smallest particles, below 20 nm in diameter, may be overestimated with this approach (**Papers IV** and **V**). Riipinen et al. (2011) reported that with around half of the total condensable organic matter condensing kinetically to nanoparticles – and the other half thermodynamically, according to particle mass – observed growth of these particles could be reproduced. This type of semi-empirical approach is used e.g. by Makkonen et al. (2014). A further improved size-dependent particle growth parameterization is introduced in **Paper IV** (see Sect. 4.3).

3 Experimental methods and data analysis

3.1 Volatility measurements

Volatilities of both laboratory-generated and ambient aerosol particles have been widely studied (**Papers I-III**; Kalberer et al., 2004; Wehner et al., 2004; Wehner et al., 2005; An et al., 2007; Ehn et al., 2007; Huffman et al., 2009a; Huffman et al., 2009b; Birmili et al., 2010; Lee et al., 2010; Hong et al., 2014). These measurements provide indirect information on the chemical composition and origin of the aerosol. To reproduce the observed multicomponent aerosol volatility from first principles, the p_{sat} values of individual aerosol constituents as well as the p_{eq} of the mixture should be known. Unfortunately, information of the p_{sat} values of low-volatility and extremely low-volatility organic compounds (see Table 1) is scarce. This is because of experimental limitations due to low gas-phase concentrations of these compounds. p_{sat} and ΔH_{vap} values of dicarboxylic acids, which is a group of semivolatile and atmospherically relevant compounds, have however been studied extensively with various techniques (Bilde et al., 2003; Chattopadhyay and Ziemann, 2005; Saleh et al., 2008; Booth et al., 2009; Saleh et al., 2009; Bilde et al., 2015). Hence, dicarboxylic acids are suited for evaluating the performance of novel methods developed for quantification of the volatility of organic species (e.g. in **Paper II** and **III**).

In this work we have applied methods that are used to determine aerosol volatility by probing changes in the particulate phase (**Paper I**; Wehner et al., 2002; Philippin et al., 2004; Ehn et al., 2007; Saleh et al., 2008) or in the gaseous phase (**Papers II and III**; Chattopadhyay and Ziemann, 2005; Cappa et al., 2007; McNeill et al., 2007; Sareen et al., 2010) upon heating the aerosol. In the former approach, aerosol particle size/volume is measured both in ambient conditions and after passing through a heated flow tube (often referred to as thermodenuder, TD). The latter approach typically uses thermal desorption to volatilize the aerosol and measures the changes in the aerosol gas-phase composition using mass spectrometry. Thermal desorption can be done at atmospheric pressure with a heated flow tube in front of the mass spectrometer as in **Papers II** and **III** or using a heated particle collector or vaporizer within the instrument (Chattopadhyay and Ziemann, 2005; Williams et al., 2006; Cappa et al., 2007; Holzinger et al., 2010; Lopez-Hilfiker et al., 2014). Both particle- and gas-phase approaches to determine aerosol volatility have their advantages – particle-phase based methods obtain the overall volatility of the aerosol while gas-phase measurements give information on the volatilities of individual compounds. When applied alone, particle-based methods are missing the information that gas-phase measurements provide and vice versa. With gas-phase measurements, only compounds that volatilize at the temperatures used are observed, i.e. non-volatile compounds are not detected unlike with the particle-phase based methods. With methods using an heated flow tube, aerosol residence time within the flow tube becomes crucial when interpreting the data, i.e. determining volatility (An et al., 2007; Riipinen et al., 2010). In **Papers I- III**, both particle-

phase and gas-phase based approaches have been separately applied. The specific approaches applied in this work are described below.

3.1.1 VDMPS for particle-phase measurements

The schematics of the main instruments, twin-DMPS (Differential Mobility Particle Sizer, Aalto et al., 2001) and VDMPS (Volatility Differential Mobility Particle Sizer, Ehn et al., 2007) used in **Paper I** are presented in Fig. 2. Twin-DMPS determines the number size distribution of ambient particles from 3 nm up to 1 µm in diameter in dry conditions by selecting parts of the aerosol size spectrum based on particle electrical mobility with a DMA (Differential Mobility Analyzer), and optically measuring the concentration of the selected particles using a CPC (Condensation Particle Counter). The VDMPS consists of a TD that heats the aerosol flow at a certain temperature and a DMPS system that determines the size distribution of the particles remaining after heating.

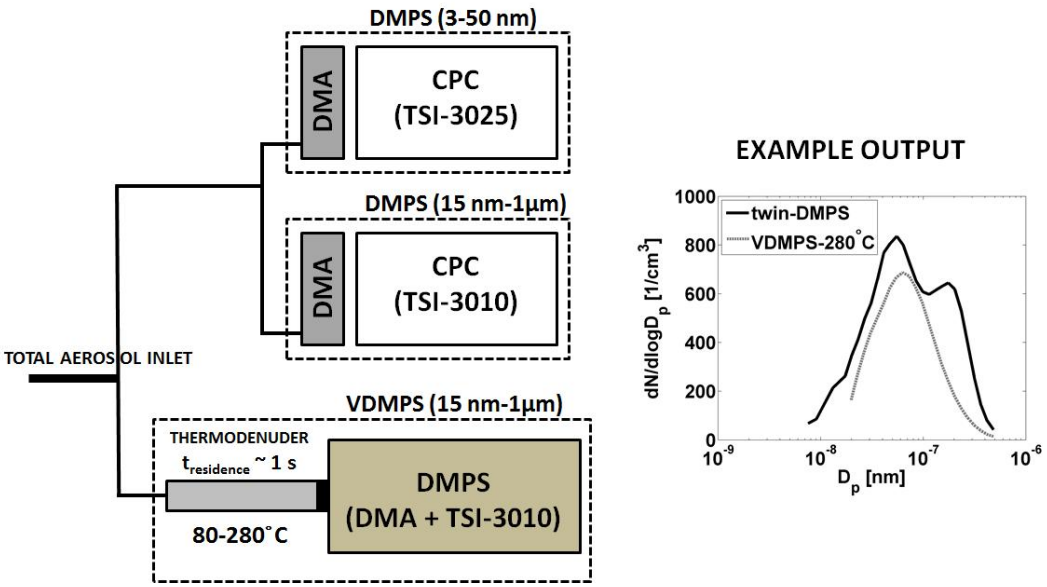

Figure 2: A schematic illustrating the setup for determining aerosol volatility – parallel measurements of ambient and heated aerosol number size distributions using twin-DMPS (Differential Mobility Particle Sizer) and VDMPS (Volatility Differential Mobility Particle Sizer) that combines a thermodenuder and a DMPS. Median ambient and heated (280 ˚C) particle number size distributions using data collected during winters 2008-2010 (adopted from **Paper I**) is presented as an example instrumental output.

The TD of this study was a 50 cm long tube made of stainless steel with an average aerosol residence time of 1.2 s. In **Paper I**, the VDMPS covered particle sizes from 20 nm up to 1 µm. Time resolution of both the VDMPS and twin-DMPS was 10 min. Due to issues

related to the VDMPS measurements – the VDMPS was occasionally affected by partially evaporated coarse mode particles that were not seen with the twin-DMPS – size range of 20-500 nm was selected for further analysis both for VDMPS and DMPS.

The VDMPS measurements for **Paper I** were performed from January 2008 to May 2010 at a rural continental background site at SMEAR II (Station for Measuring Ecosystem-Atmosphere Relations II) located in Hyytiälä in Southern Finland (Hari and Kulmala, 2005). During the first year and half (01/2008 – 04/2009), the VDMPS was in a temperature-scanning mode heating the aerosol at six different temperatures: 80, 120, 160, 200, 240 and 280 ˚C. From July 2009 onwards the VDMPS was set to heat the aerosol at constant temperature, 280 ˚C. During the latter measurement period the focus was on the non-volatile residual of the aerosol. Overall, the long-term data set with data coverage of 75% provided insights into the seasonal changes in aerosol volatility.

3.1.2 TPD aerosol-CIMS for gaseous-phase measurements

In TPD aerosol-CIMS (Temperature Programmed Desorption Aerosol Chemical Ionization Mass Spectrometer) aerosol particles are passed through a heated flow tube inlet and the volatilized chemically ionized organic compounds are detected with a quadrupole mass spectrometer (McNeill et al., 2007; Sareen et al., 2010). The changes in the gas-phase signal are then monitored upon heating the aerosol. The experimental setup for the TPD aerosol-CIMS experiments used in **Papers II** and **III** is illustrated in Fig. 3.

The volatilization flow tube was a stainless steel tube of 23 cm in length (inner diameter of 1.08 cm) with a heating tape wrapped around it. Aerosol flow of 1.8 L min^{-1} through the heated inlet lead to an aerosol residence time of around 0.7 s. The temperature in the flow tube was increased step-wise from room temperature up to around 160 ˚C. At each temperature, the monitored gas-phase signal of interest was allowed to stabilize prior to increasing the temperature in the flow tube – stabilization of the signal took around 30-90 minutes.

Volatilized aerosol material was chemically ionized in the CIMS using a negative parent ion I^- (m/z 127.0±0.2). I^- ions were produced via methyl iodide (CH_3I) passing through a radioactive alpha source. The formed ion clusters were guided from around 1 mTorr pressure to ultrahigh vacuum (10^{-8} Torr), and their mass-to-charge (m/z) ratios were detected with a quadrupole mass spectrometer. Peak or peaks in the CIMS-spectra, if fragmentation or thermal decomposition occurred, related to the studied aerosol organics were determined by comparing background spectra to the aerosol spectra. The changes in the signal of the selected peaks were monitored upon heating (see Fig. 3 as an example). Background signal was removed from the traced signal prior to data analysis.

For the TPD aerosol-CIMS experiments of **Paper II** submicron aerosol particles were generated by atomizing aqueous solutions containing organic acid and inorganic salt with varying organic acid molar fractions in the total solute (F_{org} = 0.2-0.5). The organic acids – acetic acid (AA), succinic acid (SA), oxalic acid (OxA) and citric acid (CA) – were mixed

with sodium chloride (NaCl) and ammonium sulfate (AS). In **Paper III** OxA-$CaCl_2$ aerosol was prepared via reactive uptake of oxalic acid to $CaCl_2$ particles in an aerosol flow tube reactor – oxalic acid molar fraction was estimated to be 0.1-0.2. In addition, pure sodium oxalate (Na_2Ox) aerosol was generated from aqueous solution for comparison purposes (**Paper III**). After generation, the aerosol was dried with a diffusion dryer – RH of the flow was kept below 12%. Number size distributions of the dried particles were determined using a SMPS (Scanning Mobility Particle Sizer) that has a similar working principle as a DMPS (see Section 3.1.1). With the organic acid-inorganic salt mixtures, only the organic acid partitioning to the gas-phase was detected with the TPD aerosol-CIMS. Organic salts (e.g. Na_2Ox) were detected as the corresponding organic acid in the CIMS. The residence time between the atomizer and the volatilization flow tube was around 5 s. This was the maximum time for particulate-phase reactions to take place in the aerosol mixtures prior to entering the TPD aerosol-CIMS.

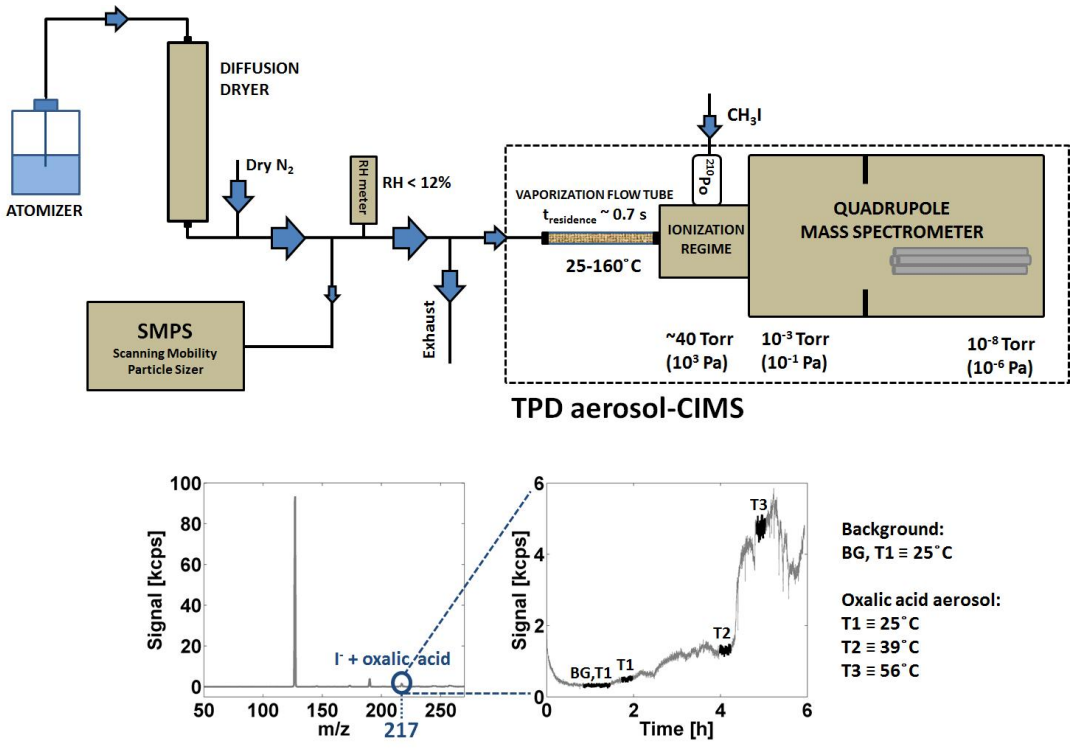

Figure 3: A schematic presenting the setup for the volatilization of dry aerosol particles and detection of aerosol gas-phase material using TPD aerosol-CIMS. As an example of typical output data upon investigation of evaporation of an organic acid aerosol (oxalic acid), molecular mass spectra and signal-trace during aerosol heating are illustrated. In the analysis averages of stabilized signals were used.

3.2 Quantitative assessment of the volatility of aerosol constituents from measurements

3.2.1 Methods based on experimental data

VFR (volume fraction remaining), i.e. the amount of aerosol material left after heating, is often used to describe aerosol volatility with measurement methods probing changes in the particle size or total volume (or mass) upon heating. In **Paper I** VFR was determined using both the VDMPS and DMPS data by calculating the total volume of the aerosol before ($V_{\mathrm{tot,DMPS}}$) and after ($V_{\mathrm{tot,VDMPS}}$) heating:

$$\mathrm{VFR} = \frac{V_{\mathrm{tot,VDMPS}}}{V_{\mathrm{tot,DMPS}}} = \frac{M_{\mathrm{tot,VDMPS}}}{M_{\mathrm{tot,DMPS}}}. \quad (6)$$

For further analysis it was assumed that VFR corresponds to MFR (mass fraction remaining), where $M_{\mathrm{tot,DMPS}}$ and $M_{\mathrm{tot,VDMPS}}$ are the total aerosol mass before and after heating, respectively, by assuming constant aerosol density of 1.6 g cm^{-3}.

For measurements probing changes in the gas-phase equilibrium upon aerosol heating, a simple way to determine the effective vaporization enthalpy ΔH_{vap} of an aerosol constituent is to apply Clausius-Clapeyron equation. In this type of approach, ΔH_{vap} is assumed to be constant in the studied temperature range. Using data from TPD aerosol-CIMS, the equation can be written as follows

$$\ln\left(\frac{p_{\mathrm{sat,i}}(T_2)}{p_{\mathrm{sat,i}}(T_1)}\right) \equiv \ln\left(\frac{\mathrm{signal}(T_2)}{\mathrm{signal}(T_1)}\right) = -\frac{\Delta H_{\mathrm{vap}}}{R}\left(\frac{1}{T_2} - \frac{1}{T_1}\right), \quad (7)$$

where signal(T) is the average signal observed at average temperature T in the volatilization flow tube and corresponds to saturated gas-phase concentration ($p_{\mathrm{sat,i}}$ via Eq. 3) of the evaporating aerosol constituent i (**Paper III**; Ortiz-Montalvo et al., 2014). If the aerosol constituent, however, does not have enough time to reach gas-particle equilibrium in the volatilization flow tube, i.e. $p_{\mathrm{eq,i}}(T) \neq p_{\mathrm{i}}(T)$ (see Riipinen et al., 2010), this approach gives only a low-end estimate for ΔH_{vap}. Similarly, concerning VFR calculations, if the particles do not reach equilibrium within the thermodenuder, the obtained VFR values are overestimations (An et al., 2007; Lee et al., 2010). Hence, the estimated aerosol volatilities depend on the residence times used and therefore may not describe the actual volatility of the studied species/aerosol. To account for non-equilibrium conditions within the flow tube for more accurate estimates of aerosol volatility, evaporation kinetics should generally be accounted for. In this work, this was done by applying the mass-transfer model by Riipinen et al. (2010) for data interpretation in **Papers I** and **II**.

3.2.2 Methods coupling experimental data with mass-transfer model

The kinetic mass-transfer model determines time-dependent evaporation of aerosol within a heated flow tube with a given residence time by solving Eq. 1, and accounting for the transition regime correction. In this work we assumed a monodisperse aerosol population

with the total particle mass concentration derived from the aerosol size distribution measurements. p_{sat} at 298 K and ΔH_{vap} of the aerosol constituents were then determined by searching the combination of these values that reproduced the measured thermogram (VFR as a function of temperature) or the normalized signal of TPD aerosol-CIMS as a function of temperature. In **Paper II** this method combining TPD aerosol-CIMS data with the kinetic evaporation model was introduced for quantifying the volatilities of organic aerosol constituents. The performance of the method was evaluated with laboratory-generated pure-component dicarboxylic acid aerosols (example data and model output shown in Fig. 4A). The results of the evaluation are discussed in detail in Section 4.2.1.

Modeling multicomponent systems, especially ambient aerosol, is challenging due to lack of information on the properties (e.g. saturation vapor pressure and surface tension) and amount of individual organic aerosol constituents as well as their aerosol-phase interactions (Topping et al., 2007). In principle, the volatilities of individual aerosol constituents can be derived from the TPD aerosol-CIMS data (McNeill et al., 2007; Sareen et al., 2010; Ortiz-Montalvo et al., 2014) with the restriction that effectively non-volatile aerosol constituents cannot be directly observed with this instrument. Particle-phase based instruments (e.g. VDMPS) measures what is left in the aerosol after heating, including the effectively non-volatile particle fraction, but separation between individual aerosol constituents is challenging. However, some indications of the composition of the aerosol residual can be obtained with additional independent data sets as was done in **Paper I**.

In **Papers I-II** a two-component approach was applied to estimate the volatilities of multicomponent systems. It should be noted that especially in the case of ambient aerosol particles this approach gives only a rough estimation on aerosol volatility. In the two-component approach aerosol particles were assumed to be composed of entirely non-volatile (p_{sat} = 0) material and material that evaporates (at least partially) within the temperature range used. The aim was to determine the volatility of the evaporating aerosol fraction (**Paper I**). The two-component approach was also used to quantify the fraction of evaporating organic matter converted to effectively non-volatile organics upon particulate-phase reactions in **Paper II.** This was done by taking advantage of the fact that the TPD aerosol-CIMS cannot detect non-volatile aerosol compounds since they prefer to stay in the particle phase. In this analysis, the inorganic salt and the formed low-volatility organic material were lumped under "non-volatile aerosol fraction". The properties of the organic acid were given to the evaporating aerosol fraction while for the non-volatile aerosol fraction the properties of the inorganic salt were given, for simplicity.

The molar fraction of the evaporating organic material in the dried aerosol ($F_{org,model}$) was obtained by reproducing the measured organic acid evaporation from the mixture – in more detail, the difference between the ratio of CIMS-signals (organic acid signal from mixture aerosol vs. that from pure-component organic aerosol) and the corresponding ratio of modeled evaporated masses (mixture vs. pure) was minimized (Fig. 4B and C). If $F_{org,model}$ was equal to F_{org}, no aerosol processing upon drying occurred. However, as was often the case, $F_{org,model}$ was lower than F_{org} indicating that part of the initial organic acid amount was converted to effectively non-volatile organic material. The fraction of the initial organic acid

molar fraction sequestered as "non-volatile" organics upon drying was defined as NVF (non-volatile fraction) and estimated as follows

$$\mathrm{NVF} = \frac{F_{\mathrm{org}} - F_{\mathrm{org,model}}}{F_{\mathrm{org}}}. \quad (8)$$

In **Paper II** two important assumptions were made concerning the above presented analysis method (Eq. 8). First of all, it was assumed that the particles, right after generation, have the same F_{org} as in the aqueous solution. This assumption has been shown to hold well for similar systems as the one applied here (Yli-Juuti et al., 2013b). It was also assumed that

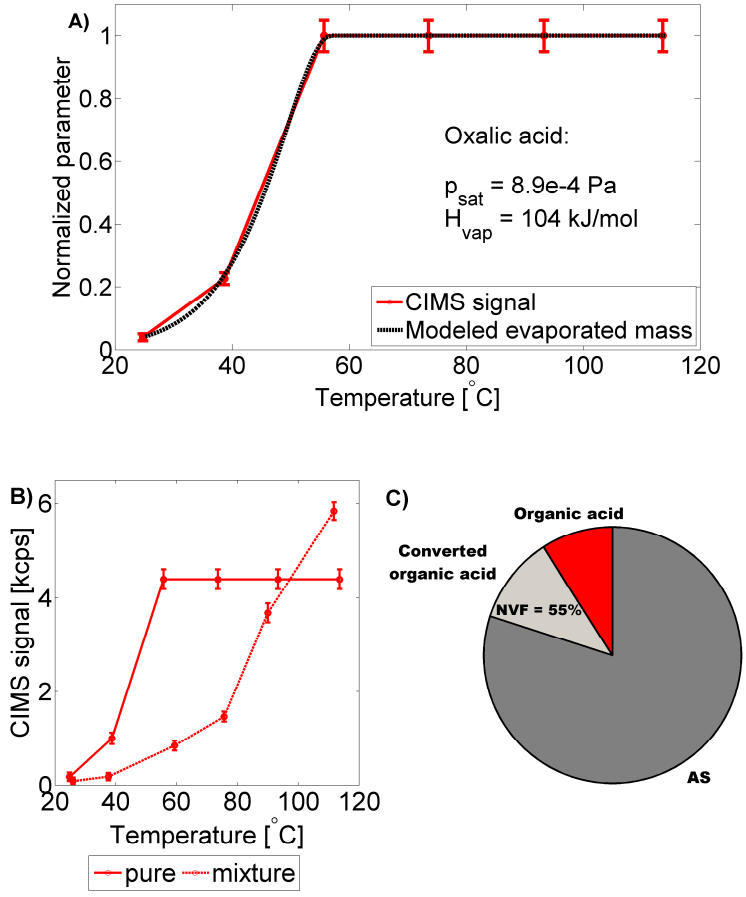

Figure 4: A) Measured evaporation of pure organic acid aerosol (oxalic acid as an example case) reproduced with the kinetic model by searching an optimum combination of p_{sat} at 298 K and ΔH_{vap}. B) Oxalic acid signals obtained upon heating pure OxA and OxA-AS aerosol mixture with initial F_{org} = 0.2. C) Pie chart describing the molar fractions of OxA, OxA sequestered as low-volatility organic matter and AS when entering TPD aerosol-CIMS. In this example 55% of the initial OxA amount was converted to low-volatility organics via aerosol processing. To note, pure OxA signal did not show changes above around 60 ˚C indicating that OxA particles were completely volatilized at those temperatures.

the organic acid in the mixtures does not evaporate significantly (maximum ~20% change in aerosol organic acid mass) upon drying the aerosol prior to TPD aerosol-CIMS. This assumption can be made if the organic acid is of relatively low-volatility, and with low F_{org}. SA and OxA (and CA) were deemed to be low-volatility enough with $F_{org} = 0.5$ and below – only around 10% decrease in NVF was estimated using the kinetic model.

3.3 Experimental data used for nanoparticle growth parameterization

To design the semi-empirical parameterization of nanoparticle growth in **Paper IV**, the experimental data on aerosol particle number size distributions from continental measurement stations was utilized. The data was grouped to three size bins: 1.5-3 nm, 3-7 nm and 7-20 nm, and particle growth rates (GRs) were calculated from the measured ambient air ion/ particle number size distributions following the method introduced by Hirsikko et al. (2005) and Yli-Juuti et al. (2011). The observed GR for a given size bin with d_p representing the midpoint of the size bin was converted to the total aerosol mass flux with Eq. 5, which was then used as the basis of the parameterization (see Sect. 4.3 for details). GR data used in **Paper IV** was obtained from Hyytiälä during 2003-2009 (Yli-Juuti et al., 2011) and from five other European sites – Melpitz and Hohenpeissenberg in Germany, Vavihill in Sweden, Finokalia in Greece and K-puszta in Hungary – during 2008-2009 (Manninen et al., 2010).

4 Results and discussion

4.1 Volatility of boreal forest aerosol

Boreal forest particles showed a smooth thermogram as expected for aerosol that consists of wide range of species with differing volatilities, in qualitative agreement with previous research (see Fig. 6 in **Paper I**). On average 19% of the boreal forest aerosol volume (or mass) was non-volatile at 280 ˚C. This MFR is comparable to a measured MFR of oxidized organics (15-20% of aerosol organic mass left at around 240 ˚C, Huffman et al., 2009a). Urban aerosol is likely to be less volatile (22-30% of aerosol mass left at around 300 ˚C, Backman et al., 2010; Birmili et al., 2010) and freshly formed organics more volatile (only 10% of aerosol mass left at 140 ˚C, Lee et al., 2010) than the boreal forest aerosol. However, varying residence times and aerosol type between our study and other relevant studies complicated direct comparisons in this regard. By applying the kinetic evaporation model, the volatility of the boreal forest aerosol was given a quantitative estimate by assuming two-component aerosol. For the evaporating aerosol fraction $p_{sat} = 10^{-6}$ Pa was obtained. This is a reasonable value in describing the average volatility of the evaporating aerosol material, organics and inorganics alike, in submicron aerosol (see Sect. 2.1 and e.g. Donahue et al., 2006).

Seasonal dependency in aerosol volatility was found: the VFR at 80-280 ˚C was the lowest during summer months and the highest during winter. Number size distributions of ambient (DMPS) and heated (VDMPS at 280 ˚C) aerosol particles were compared (see Fig. 2 as an example). The DMPS distributions were bi- or trimodal with one/two Aitken (25-100 nm) and one accumulation (100-500 nm) modes comparable with Dal Maso et al. (2005), while the VDMPS distributions were monomodal. This was probably because a large fraction of the smallest aerosol particles evaporated below the detection limit of VDMPS (20 nm) upon volatilization.

As mentioned above, significant volume fraction of the aerosol in the boreal environment was non-volatile in agreement with other studies (Kalberer et al., 2004; Wehner et al., 2004; Wehner et al., 2005; Ehn et al., 2007; Backman et al., 2010; Birmili et al., 2010; Ehn et al., 2014). Upper limit estimate for BC contribution to sub-500 nm aerosol mass was determined from aethalometer (Hansen et al., 1984) measurements by assuming that all BC mass is in sub-500 nm particles. The highest BCF (black carbon mass fraction) was observed during winter and fall months (13-15% of the total aerosol mass). At maximum black carbon explained 55-87% of the non-volatile residual depending on the season: during winter the contribution of BC was the smallest and during summer the highest. However, for summer the correlation between BCF and MFR at 280 ˚C was poor (linear correlation coefficient $R = 0.34$, $p = 10^{-3}$) while being notably better for other seasons ($R > 0.5$, $p < 10^{-5}$). This indicates that in the summer larger fraction of BC was in larger particles (> 500 nm) as compared with the other seasons, suggesting long-range transport as the primary BC source in the summer vs. fresh emissions of BC from local sources during the colder months.

Sea salt and crustal material are not considered to have a notable contribution to the non-volatile residual in sub-500 nm particles in an inland region (Saarikoski et al., 2005). Hence, the results suggest that organic compounds may be important in explaining the non-BC fraction of the non-volatile residual. Similar conclusions were made by Backman et al. (2010) who investigated the volatility and light-scattering properties of the non-volatile residual in urban aerosols.

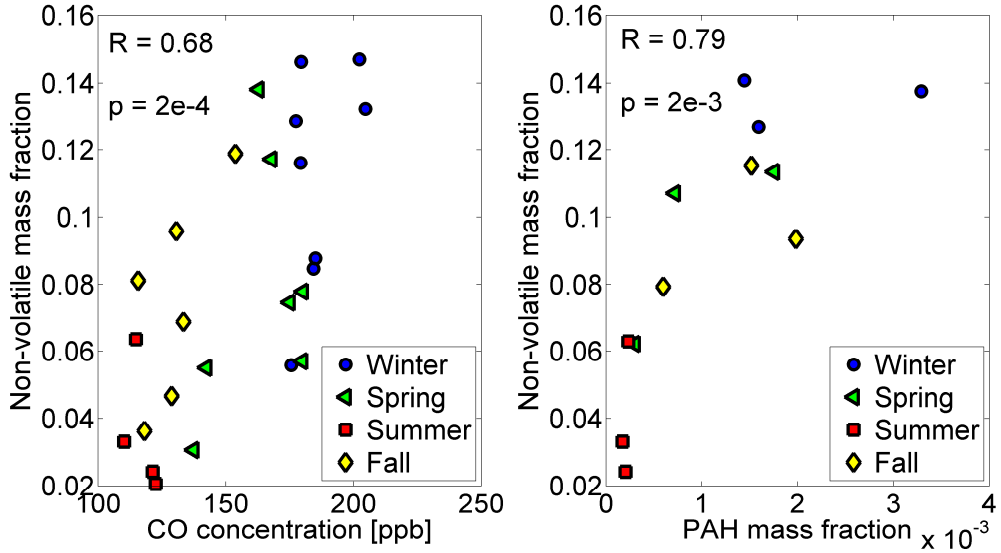

Figure 5: Non-volatile (not evaporating at 280 ˚C) aerosol mass fraction excluding the contribution of BC is presented against concentrations of anthropogenic pollutants CO (left panel) and PAH (right panel) during different seasons and years. There are less data points in the PAH analysis since monthly PAH concentrations (converted to mass fractions with the help of DMPS data) were determined only from year 2009 filter samples. Pearson correlation coefficients (R) and the significance of the correlation (p) are also given.

The maximum mass contribution of BC was removed from the aerosol residual ($MFR_{non\text{-}BC}$), and the obtained $MFR_{non\text{-}BC}$ was correlated with meteorological parameters, concentrations of anthropogenic trace gases, mass concentrations of particulate pollutants (polycyclic aromatic hydrocarbons, PAHs) and aerosol constituents obtained from aerosol mass spectrometer (AMS, Jayne et al., 2000). Aerosol mass spectra were measured at two campaigns in late spring and early fall of 2008.

Negative correlation between $MFR_{non\text{-}BC}$ and ambient temperature was found (R = -0.5, $p < 10^{-5}$) whereas the correlation between $MFR_{non\text{-}BC}$ and solar radiation was not as clear (R = -0.3, $p < 10^{-5}$). This suggests that high $MFR_{non\text{-}BC}$ at low temperatures compared to lower $MFR_{non\text{-}BC}$ at higher temperatures is not solely explained by the changes in the boundary layer height but rather due to different particle and vapor sources between warm

and cold seasons. For example, pollutant concentrations, e.g. of CO and PAHs, were observed to be higher during cold months than during summer likely due to higher anthropogenic emissions from e.g. residential heating. Overall, strong positive correlation between $MFR_{non\text{-}BC}$ and these anthropogenic pollutant markers was observed (Fig. 5). However, the correlations were not as clear for each season separately. This suggests that while anthropogenic organic compounds can have an important contribution to the non-volatile non-BC aerosol residual, organic compounds of natural origin should also be considered.

The AMS data provided further insight into the potential origin of the $MFR_{non\text{-}BC}$. For analysis purposes, aerosol nitrate mass fraction was divided to inorganic nitrate (bound to ammonia) and organic nitrate. During the fall campaign around half of the aerosol nitrate was estimated to be organic. The correlation of $MFR_{non\text{-}BC}$ with the organonitrate mass fraction was 0.55 ($p = 2 \cdot 10^{-4}$) and with aerosol organic mass fraction 0.29 ($p = 2 \cdot 10^{-3}$). High organonitrate mass fractions (and high $MFR_{non\text{-}BC}$) were associated with both clean and more polluted air masses indicating both natural and anthropogenic influence. To note, organonitrates determined from the mass spectrometer data should be rather called organic nitrogen-containing compounds. Therefore, e.g. amines/aminium salts (Smith et al., 2010), if present, are likely part of the "organonitrate" aerosol fraction.

Important pathway for organonitrate formation in the atmosphere is nighttime chemistry between BVOCs and anthropogenic oxidants (Fry et al., 2009; Hao et al., 2014). The contribution of organonitrates in the aerosol particles depends on the location – in some regions organonitrates can explain only a small fraction of the total nitrate mass while in other regions it can exceed the amount of inorganic nitrate (Hao et al., 2014). In **Paper I** the estimated organonitrate mass fraction was 3-5% which is comparable to the inorganic nitrate mass fraction. Fry et al. (2009) estimated saturation vapor pressure of around $7 \cdot 10^{-4}$ Pa for condensing organonitrate species formed upon β-pinene oxidation with nitrate radical in chamber experiments. Hao et al. (2014) reported that while most of the aerosol phase organonitrate is associated with SV-OOA (semivolatile oxidized organic aerosol, cf. Table 1) via ambient measurements, a notable fraction, around 20%, can be linked to LV-OOA (low-volatility oxidized organic aerosol, cf. Table 1). However, whether these low-volatility organonitrates or fraction of them can survive in the particulate phase after heating to 280 ˚C or not is still an open question.

The chemical composition of the non-volatile aerosol residual depends on ambient conditions, aerosol and vapor sources, and hence, the time of year. The residual can contain both anthropogenic and biogenic organics in addition to BC. Some organic compounds of biogenic origin, e.g. organonitrates, are formed under anthropogenic influence meaning that they cannot be completely separated from human activities. As indicated in **Paper I**, these compounds may contribute to the observed non-volatile aerosol residual in Hyytiälä.

4.2 Volatility of organic acid - inorganic salt aerosol mixtures

4.2.1 Evaluating TPD aerosol-CIMS performance with pure organic acids

In **Paper III**, the volatility of pure oxalic acid was determined using Eq. 7, yielding an effective ΔH_{vap} = (85±12) kJ mol^{-1}. With the same data set, data analysis with the kinetic model (see Sect. 3.2.2) yielded oxalic acid p_{sat} = 9·10^{-4} Pa (uncertainty range from 4·10^{-4} to 2·10^{-3} Pa) at 298K with ΔH_{vap} = 104 kJ mol^{-1} (from 88 to 146 kJ mol^{-1}) (**Paper II**). These results, together with the model calculations suggest that oxalic acid aerosol (volumetric mean diameter of 106 nm and an average aerosol mass concentration of 4.3 µg m^{-3}) did not reach equilibrium in the system upon heating within residence time of around 1 s. If given enough time (around 40 s), these particles would completely evaporate already at room temperature.

The volatility estimates of organic acids vary considerably between studies. Two orders of magnitude differences in p_{sat} and 50 kJ mol^{-1} differences in ΔH_{vap} exist between the reported values (Bilde et al., 2015, and references therein). The discrepancies have been associated with e.g. differences in the particle phase state due to differences in the sample generation and preparation techniques, as well as due to the measurement methods themselves (Bilde et al., 2003; Soonsin et al., 2010). The phase state of the dried aerosol is likely to play a role also in our study, as the determined p_{sat} and ΔH_{vap} varied between individual experiments. Less than an order of magnitude differences in p_{sat} and 20-40 kJ mol^{-1} differences in ΔH_{vap} were observed (**Paper II**). Since the same instrumental setup was in use throughout the experiments, changes in the generated aerosol are likely to explain the observed differences. Residual water in the aerosol after drying may affect the measured thermodynamic properties of the organic acid, and result in lower ΔH_{vap} and higher p_{sat} values (Cappa et al., 2007). However, it should be noted that also opposing results exist (Saleh et al., 2010). In general, the estimated volatilities of the studied organic acids (OxA, SA and CA) were in the range of literature values demonstrating that the instrument and analysis method alike perform well.

4.2.2 Organic salt formation

Partitioning of organic acids in the presence of inorganic salts was investigated by comparing organic acid evaporation from the mixtures containing inorganic salts to that from pure-component aerosol. Pure vs. mixture evaporation is illustrated for oxalic acid in Fig. 4B. SA, OA and CA continued to evaporate from the mixtures beyond temperatures where the pure organic acid aerosol reached complete evaporation. This suggests that organic acid partitioning is enhanced in the presence of inorganic salts.

Raoult's law states that the equilibrium vapor pressure of an organic acid is lowered over a mixture (see Eq. 2). To determine whether the observed enhancement in the organic acid partitioning in the organic-inorganic aerosol (**Papers II** and **III**) was due to aerosol

processing or simply due to low molar fraction of the organic acid in the aerosol, the kinetic model was applied.

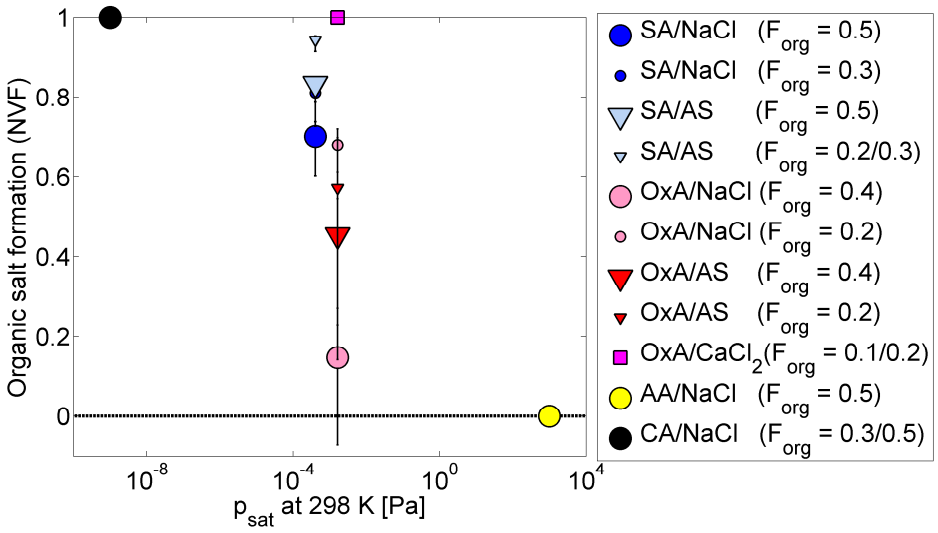

Figure 6: The fraction of the initial organic acid amount converted to effectively non-volatile organic salts (NVF) upon particle drying with different initial F_{org} as a function of the saturation vapor pressure of pure organic acid. Marker sizes depict F_{org} – smaller marker with lower F_{org} in the organic acid-inorganic salt aerosol. Dashed black line represents NVF = 0, i.e. the limit where no organic salt formation occurs. Figure is adopted from **Paper II** and data set from **Paper III** (OxA/$CaCl_2$ aerosol) is applied. SA: succinic acid, OxA: oxalic acid, AA: acetic acid, CA: citric acid and AS: ammonium sulfate.

Analysis combining the TPD aerosol-CIMS data with the kinetic model indicated that the observed enhancement in SA and OxA partitioning in the presence of monovalent inorganic salts was indeed due to particulate-phase processing, as nonzero NVF was obtained (see Sect. 3.2.2 and **Paper II**). We suggest that the formed low-volatility organic matter is organic salt (see discussion in Sect. 4.2.3). Due to limitations in AA and CA data, the magnitude of organic salt formation within mixtures of NaCl with these organic acids was only qualitatively estimated. Acetic acid evaporated from the AA-NaCl aerosol as much as from the pure AA aerosol indicating no organic salt formation (NVF = 0). Minimal evaporation of citric acid from CA-NaCl aerosol was observed only at temperatures above 100 ˚C while CA started evaporating from pure-component organic aerosol at around 60 ˚C. Hence, complete organic acid conversion was assumed for CA-NaCl aerosol (NVF = 1) in accordance with Laskin et al. (2012). In Fig. 6 the average fraction of the organic acid sequestered as low-volatility organic matter (NVF) with different initial F_{org} is presented against p_{sat} of the pure-component organic acid. NVFs obtained both from the quantitative and qualitative analysis are illustrated. According to our study, aerosol processing took place

within mixtures of monovalent inorganic salts and organic acids with $p_{sat} \leq 10^{-3}$. More processing occurred with lower F_{org} in accordance with Zardini et al. (2010) and Yli-Juuti et al. (2013b).

In **Paper III**, the formation of low-volatility oxalates within oxalic acid-divalent inorganic salt ($CaCl_2$, $ZnCl_2$ and $MgCl_2$) mixtures was demonstrated by measuring the evaporation of oxalic acid from OxA-$CaCl_2$ aerosol – the onset temperature for oxalic acid evaporation was as high as 100 ˚C. In the case of OxA-$CaCl_2$ aerosol, kinetic model calculations suggest that over 90% of the oxalic acid was converted to calcium oxalate (not presented in the papers). For comparison, within oxalic acid-monovalent inorganic salt mixtures of similar initial F_{org}, around 55-75% of the oxalic acid was converted. Hence, organic salt formation within organic acid-divalent inorganic salt aerosol may be enhanced over that within monovalent inorganic mixtures. Monovalent cations – especially Na^+ from NaCl and NH_4^+ from $(NH_4)_2SO_4$ – are considered to be important aerosol inorganic constituents globally while the contribution of divalent cations – for example Mg^{2+} and Ca^{2+} – is significant in sea salt, in a form of $CaCl_2$ and $MgCl_2$, and in mineral dust ($CaCO_3$).

The effect of aerosol acidity – typical aerosol pH of around 2-5 – on the aerosol processing within the aerosol mixtures was investigated (**Paper II**). Aerosol acidity plays a role in the aerosol processing especially when semivolatile organic acids are mixed with inorganic salts. Suppressed formation of organic salts under low pH for OxA and SA mixtures was observed.

4.2.3 Discussion on volatility of organic salts

Interactions between particulate inorganic salts and organic acids and further, enhanced partitioning of the organic acid is evident (**Papers II** and **III**; Zardini et al., 2010; Laskin et al., 2012; Yli-Juuti et al., 2013b). Laskin et al. (2012) provided first direct observations of sodium organic salt formation within submicron organic acid-NaCl aerosol. Prior to this, aerosol processing within succinic acid-NaCl and -AS mixtures has been indirectly observed with low relative amounts of succinic acid (Zardini et al., 2010; Yli-Juuti et al., 2013b). Laskin et al. (2012) reported organic salt formation in organic acid-NaCl mixtures as a result of chloride depletion by the evaporation of hydrochloric acid (HCl) from the aerosol surface upon drying. They observed complete chloride depletion within CA-NaCl aerosol with initial molar ratio of 1:1 while within AA-NaCl aerosol mixtures no organic salt formation took place. In the case of acetic acid-NaCl aerosol, highly volatile acetic acid ($p_{sat,AA} \sim 10^3$ Pa, Yaws, 2003) evaporated from the particles faster than HCl.

Evaporation of HCl is not necessarily expected in bulk – no sodium salt formation has been observed in supermicron succinic acid- or malonic acid-NaCl mixtures upon drying (Ma et al., 2013). Also, fast drying process can inhibit the depletion of chloride especially from large particles. However, in the case of oxalic acid, formation of sodium oxalate can occur even when the particles are supermicron sized (Ma et al., 2013). Formation of low-hygroscopicity sodium oxalate will lead to lowering of particle water content and further promote the volatilization of HCl from the surface of OxA-NaCl particles. To compare,

sodium succinate and malonate have been reported to be hygroscopic. The results of Ma et al. (2013) are in agreement with the E-AIM (Extended Aerosol Inorganic Model, Clegg and Seinfeld, 2006b, a) calculations performed in **Paper II** for bulk SA- and OxA-NaCl mixtures – significant chloride depletion was predicted for OxA-NaCl mixtures with atmospherically relevant NaCl concentrations (1-1000 µg m^{-3}, when also supermicron sea salt particles are accounted for) but not for SA-NaCl mixtures.

Organic salt formation can partly explain why oxalic acid is highly abundant in the atmospheric organic aerosol despite of its relatively high pure-component volatility (see Fig. 4 and e.g. Bilde et al., 2015) – even the most abundant individual identified organic compound (Neusüss et al., 2000; Ervens et al., 2011 and references therein). Also, high mass concentrations of succinic acid and malonic acid in submicron atmospheric aerosol (Saxena and Hildemann, 1996; Kawamura et al., 2003; Narukawa et al., 2003; Fu et al., 2013) indicate that aerosol processing enhances the partitioning of these small-molecular weight organic acids. Typical contribution of dicarboxylic acids to the total OA mass in continental regions is few percents (Kawamura et al., 2003) while in marine environments their contribution can be as high as 20% (Fu et al., 2013). It should be noted that with analysis methods using thermal desorption, organic acids of higher volatility may be present because of thermal decomposition of larger organic molecules (Lopez-Hilfiker et al., 2015).

Concerning the volatility of sodium salts, onset temperature of evaporation of sodium oxalate was as high as 100 ˚C (**Paper III**) suggesting that at least sodium oxalate is of very low-volatility. By applying the kinetic model, rough estimate of 10^{-13} Pa at 298 K for p_{sat} of sodium oxalate was obtained (not presented in the papers).

Recent studies report that the saturation vapor pressure of ammonium oxalate is significantly lower than that of pure oxalic acid – p_{sat} of around 10^{-6} Pa for ammonium oxalate (Ortiz-Montalvo et al., 2014; Paciga et al., 2014). However, this has not shown to be the case for adipic acid vs. ammonium adipate, indicating that not all dicarboxylic acids react with ammonium to form low-volatility organic salts (Paciga et al., 2014). These observations have been associated with acid strength – stronger acid forms less volatile salt. However, as our results show, when succinic acid, which has similar volatility and acidity (K_{a1}(aq) around 10^{-5}, Haynes, 2011) as adipic acid, is mixed with AS, succinic acid partitioning is significantly enhanced.

Formation of nitrogen-containing organic compounds and organosulfates has been observed in aerosol particles containing organics (from photooxidation of terpenes, aromatics and isoprene and from reactive uptake of aldehydes, e.g. glyoxal) and ammonium sulfate (Nguyen et al., 2012; Liggio et al., 2005; Surratt et al., 2007; Lim et al., 2010). However, no direct evidence of the presence of these compounds in dicarboxylic acid-AS aerosols has been found (Yli-Juuti et al., 2013b). In the light of the recent literature, organic salt formation seems the most plausible explanation for the observed enhancement in organic acid partitioning not only in NaCl aerosol mixtures but also within the AS aerosol in this study. In the presence of water molecules, organic acid can combine with an ammonium ion and ammonium salt is formed, leaving ammonium bisulfate and hydrogen ions left

(Salorinne et al., 2014). Particulate-phase processing within organic acid-AS mixtures lowering aerosol volatility may help explaining the observed anthropogenic enhancement in SOA formation from biogenic precursors. Aminium salts have also been observed to be stable in atmospheric conditions with similar or lower volatilities than ammonium sulfate, (Barsanti et al., 2009; Smith et al., 2010), giving rise to speculations on the possible interactions between dicarboxylic acids and amines as well (Yli-Juuti et al., 2013a).

4.2.4 Discussion on hygroscopicity of organic salts

While interactions between monovalent cations and organic acids, and divalent cations and organic acids can lead to formation of low-volatility organic salts, the changes in aerosol hygroscopicity are mainly determined by the metal valency (**Paper III**). Divalent cations can react with organic acids (oxalic acid, **Paper III**) to form very low-hygroscopicity material likely due to formation of insoluble organic salt coating on the particle. Even small amounts of the insoluble material on the particle surface can significantly alter the properties of the particle (**Paper III**; Schwier et al., 2011). An insoluble surface coating may make the particles appear highly viscous or glassy, hinder aerosol evaporation and affect the uptake of atmospheric vapors (**Paper III**; Virtanen et al., 2010). On the contrary, acid-base neutralization reactions between monovalent cations and organic acids (oxalic acid-NaCl as an example, **Paper III**) are not likely to affect aerosol hygroscopicity, at least when the inorganic salt dominates the aerosol mass. If the aerosol is dominated by the organic salt, depending on the salt, aerosol can be either hygroscopic or not – for example, sodium succinate has been reported to be hygroscopic while sodium oxalate and ammonium oxalate have been deemed low-/non-hygroscopic (Peng and Chan, 2001; Ma et al., 2013).

Hence, aerosol-phase reactions between organic and inorganic species can lead to drastic changes in particle chemical properties, morphology and mass-transfer. In order to accurately describe the partitioning of organic compounds between gaseous and particulate phases, organic-inorganic reactions, e.g. organic salt formation as discussed here, may be an important addition to atmospheric models.

4.3 Semi-empirical size-dependent parameterization for nanoparticle growth

Size-dependency in the growth of sub-20 nm particles has been observed in the field – larger particles grow faster than the smaller ones (**Paper IV**; Hirsikko et al., 2005; Manninen et al., 2010; Yli-Juuti et al., 2011; Kuang et al., 2012). The size-dependency probably results from different volatilities of the condensing species as well as the effect of particle curvature on the equilibrium vapor pressure. However, the ambient concentrations of the condensing vapors may vary during new particle formation affecting the observed growth rates (Yli-Juuti et al., 2009). The growth of 3-20 nm particles shows a clear seasonal pattern while the growth of 1.5-3 nm particles is observed to be relatively constant throughout the year. The discussed features related to sub-20 nm particle growth are illustrated in Fig. 7 for Hyytiälä.

In **Paper IV** a semi-empirical parameterization was developed to capture the observed size-dependency and seasonality in sub-20 nm particle growth during new particle formation. As an improvement for the simple estimates Riipinen et al. (2011) presented (namely, that around 50% of organics condense as non-volatile), the parameterization assumes that all the condensing organic material is non-volatile but corrects for the overestimation in sub-20 nm particle growth with size-specific scaling factors. Above 20 nm sizes, kinetic organic condensation is assumed. This type of parameterization is easily applicable to atmospheric models currently treating organic condensation kinetically (Spracklen et al., 2005a; Spracklen et al., 2005b; Pierce and Adams, 2009; Makkonen et al., 2012).

Sulfuric acid plays an important role in the first steps of new particle formation (Sipilä et al., 2010; Kulmala et al., 2013) while atmospheric condensable organic compounds typically dominate particle growth, especially in rural environments (Pierce et al., 2011; Yli-Juuti et al., 2011; Riipinen et al., 2012). The developed parameterization includes particle condensational growth by sulfuric acid, biogenic organic compounds from first-order oxidation of monoterpenes (traditional BSOA-precursor) and extra-SOA (in **Paper IV** called "background"). Total condensational mass flux, I_{tot}, onto a nanoparticle with diameter of d_{p} is written as follows

$$I_{\mathrm{tot}}(d_{\mathrm{p}}) = I_{\mathrm{SA}}(d_{\mathrm{p}}) + k_{\mathrm{BSOA}}(d_{\mathrm{p}}) \cdot I_{\mathrm{BSOA}}(d_{\mathrm{p}}) + k_{\mathrm{extraSOA}}(d_{\mathrm{p}}) \cdot I_{\mathrm{extraSOA}}(d_{\mathrm{p}}), \quad (9)$$

where I_{SA} is the mass flux of sulfuric acid, I_{BSOA} is the mass flux of traditional BSOA and I_{extraSOA} is the mass flux of additional biogenic organic species associated with human activities. I_{extraSOA} was assumed not to have a seasonal pattern, for simplicity (cf. I_{BSOA} peaks during summer). Scaling factors k_{BSOA} and k_{extraSOA} describe the fractions of traditional BSOA and extra-SOA precursors that condense onto a nanoparticle of d_{p} in diameter, i.e. indirectly taking into account non-zero saturation vapor pressure of the condensing species.

Estimates for both the scaling factors (values from 0 to 1) and the amount (molecular concentration) of extra-SOA were obtained by least-square fitting Eq. 9 to ambient data separately for the three size bins. Values for k_{extraSOA} were estimated by assuming that particles of 7-20 nm are at the kinetic limit, i.e. k_{extraSOA} was set to unity for 7-20 nm particles. I_{SA} and I_{BSOA} were obtained from the corresponding molecular concentrations of sulfuric acid and the oxidation products of biogenic monoterpenes using Eq. 4 with the transition regime correction. The kinetic regime mass transfer equation was applied to the analysis since growth of particles even as small as 1.5-3 nm was investigated. From the most part, I_{SA} and I_{BSOA} were obtained from simulated concentrations of sulfuric acid and monoterpene oxidation products from GLOMAP (Global Model of Aerosol Processes, Spracklen et al., 2005a; Spracklen et al., 2005b) for the year 2008. Monthly median daytime data was used in the analysis.

Performance of the parameterization was first evaluated with Hyytiälä long-term data set. Even though the parameterization is a simplified description of reality, it was able to reproduce the observed size-dependency and seasonal behavior in sub-20 nm particle growth (Fig. 7) within a factor of 2. The variation between the GRs from the observations and from the parameterization is comparable to or smaller than the uncertainty in the

observed GRs arising from the method used for GR calculation and from the experimental uncertainties (Leppä et al., 2013).

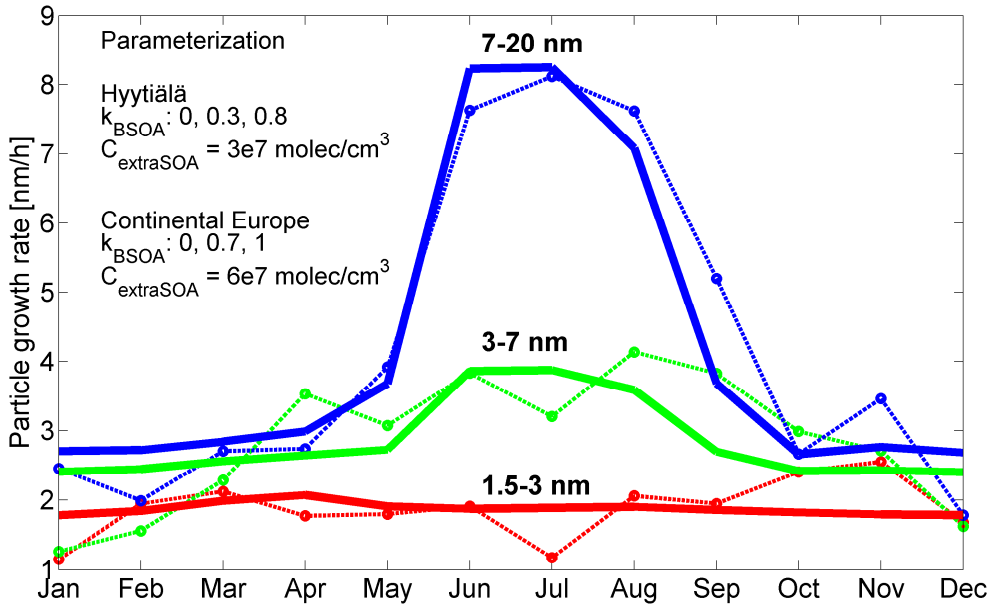

Figure 7: Growth rates of particles 1.5-3 nm, 3-7 nm and 7-20 nm obtained from observations (dashed lines with dots) and from fitting the parameterization function to ambient data, 7-year data set from Hyytiälä (solid lines). Parameters, i.e. fitting results, for the parameterization of sub-20 nm particle growth – scaling factors to slow down kinetic condensation of biogenic organics for 1.5-3 nm, 3-7 nm and 7-20 nm particles and the ambient concentration of extra-SOA – both for Hyytiälä conditions and more generally for European continental regions are presented. The figure is adapted from **Paper IV**.

Notably, sulfuric acid and traditional BSOA precursors were not able to explain alone the observed growth in any of the particle sizes. The ambient daytime concentration of the extra-SOA was estimated to be 2-4·10^7 cm^{-3}, which is comparable to that of traditional BSOA precursor (10^6-10^8 cm^{-3} depending on season). It was shown that the extra-SOA in the parameterization is comparable to an additional SOA mass source (globally 100 Tg year^{-1}) correlated with anthropogenic CO emissions, required to reproduce observed global OA concentrations (**Paper IV**; Spracklen et al., 2011). This extra-SOA would correspond to ASOA as defined in Table 1 with a global source of FSOA 10 Tg year^{-1} and eBSOA around 90 Tg year^{-1} (cf. typical global source of traditional BSOA is 10-30 Tg year^{-1}). Hence, also in a relatively clean background site like Hyytiälä, low-volatility organics related to human activities are likely be in an important role, in agreement with **Paper I**.

Scaling factors for traditional BSOA (k_{BSOA}) precursors were 0 for 1.5-3 nm, 0.3 for 3-7 nm and 0.8 for 7-20 nm. For extra-SOA precursors the scaling factors ($k_{extraSOA}$) were 0.4 for 1.5-3 nm, 0.8 for 3-7 nm and 1.0 for 7-20 nm. The results would suggest that 1.5-3 nm particles do not grow only by the condensation of traditional BSOA precursors but would require also other low-volatility organic compounds present in the winter as well. This is not in agreement with Ehn et al. (2014) who reported that ELVOCs from the oxidation of monoterpenes dominate the growth of freshly nucleated particles. The disagreement likely arises from the rough assumption made concerning the extra-SOA precursors with a constant concentration throughout the year. The concentrations of extra-SOA may be lower during summer compared to winter as shown in **Paper IV**. This type of seasonal behavior of extra-SOA would result in nonzero k_{BSOA} for particles of 1.5-3 nm. It should be also noted that the growth rates of 1-3 nm particles are difficult to determine accurately due to measurement uncertainties (Leppä et al., 2013).

GR data from five other European sites were relatively scarce. There were 17-68 data points for the other stations as compared with the 421 points for Hyytiälä. Therefore, instead of fitting the parameterization individually for each site, monthly medians GRs averaged over all the stations were used in the analysis. The scaling factors k_{BSOA} were 0 for 1.5-3 nm, 0.7 for 3-7 nm and 1.0 for 7-20 nm, and the concentration of extra-SOA precursors was estimated to be around $6 \cdot 10^7$ cm^{-3} ($k_{extraSOA}$ of 0.3, 0.8 and 1.0 for 1.5-3 nm, 3-7 nm and 7-20 nm, respectively). While the correlation between the observed and parameterized GRs was poorer with the combined data set from six sites ($R = 0.45$, $p < 10^{-5}$) than with Hyytiälä data alone ($R = 0.80$, $p < 10^{-5}$), the observed growth rates were typically captured within a factor of 2. The scaling factors were qualitatively comparable to those obtained with Hyytiälä data with k values increasing with particle size and approaching 1 for the largest particles. The required concentration of the extra-SOA precursors was slightly higher with the combined European data set, which may point to the fact that some of the sites are more affected by anthropogenic pollution than Hyytiälä. With more data per site, the parameterization could be used to assess the importance of the extra-SOA and its connection to human activities in different environments.

The relevance of the presented parameterization for particle and CCN numbers was evaluated using a global aerosol model, GEOS-Chem-TOMAS (as in Pierce et al., 2013) in **Paper V**. In addition, another size-dependent growth rate parameterization for sub-3 nm particles (Kuang et al., 2012) was separately applied to the model. To understand the importance of the organic condensation scheme on simulated CCN-sized particle numbers, both kinetic and thermodynamic approaches were tested. In addition to a global SOA source strength of 19 Tg year^{-1} (traditional BSOA from the oxidation products of terrestrial biogenic monoterpenes), extra-SOA of 100 Tg year^{-1} was applied to the model to test the significance of total organic aerosol mass burden on CCN-sized particle numbers (**Paper V**; Spracklen et al., 2011). The extra-SOA was applied to the model by spatially correlating it with the emissions of anthropogenic CO, as was also done by Spracklen et al. (2011).

Three pairs of simulations are discussed in more detail (Fig. 8). First, the condensation of traditional BSOA onto the aerosol size distribution using the ”kinetic approach” vs. the “thermodynamic approach” (defined as SURF-BASE vs. MASS-BASE, see Riipinen et al., 2011) was tested. Then, the kinetic condensation of organic matter was run with and without the extra-SOA (SURF-XSOA vs. SURF-BASE), and with and without a size-dependent particle growth parameterization (SURF-XSOA-H for sub-20 nm and SURF-XSOA-K for sub-3 nm particle growth vs. SURF-XSOA). Further, the simulation results were compared with ground-based measurements of submicron aerosol size distributions from 21 sites with varying characteristics around Europe and North-America.

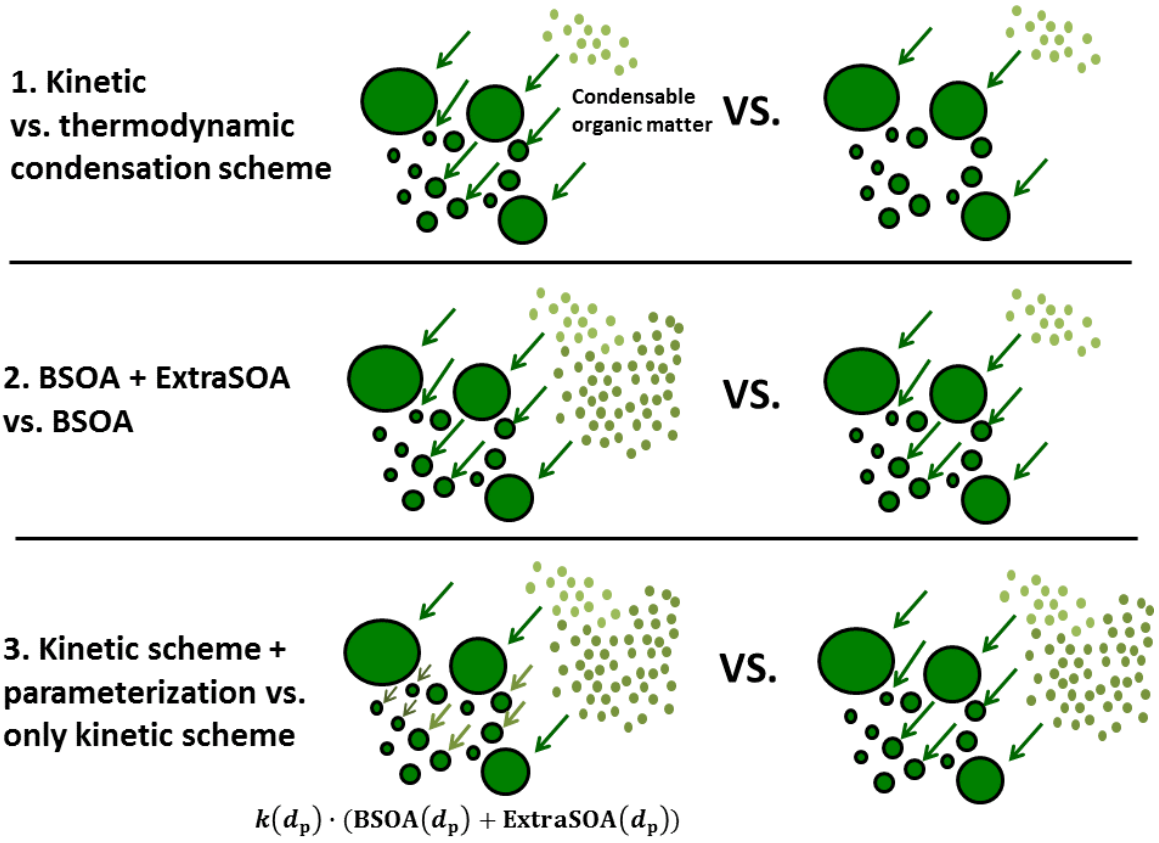

Figure 8: Illustration of three simulation pairs (cf. Table 2) from **Paper V**: 1. Traditional biogenic organic matter condensed onto particle size distribution according to particle surface area (kinetic approach) vs. mass (thermodynamic approach), 2. Kinetic condensation of organic matter with and without extra-SOA and 3. Kinetic organic condensation with extra-SOA, with and without the size-dependent growth parameterization of sub-20 nm particles (*k* is a size-dependent scaling factor to slow down the kinetic organic condensation illustrated in the figure with different sized and colored arrows).

The change in the annual mean particle number concentration between the two simulations was determined – ΔN40 was selected as a proxy for small CCN-sized particles, > 40 nm in diameter (Table 2). There was a global increase of around 11% in N40 when organic matter (traditional BSOA) was condensed relative to particle surface area compared to the mass-based condensation simulation. In biogenically active areas near the equator the increase typically exceeded 50%. When comparing the simulated aerosol number size distributions with the measured ones, both condensation schemes typically lead to overestimation in sub-10 nm particle numbers and underestimation in CCN-sized particle numbers.

Table 2: Annual global mean and maximum absolute local change in the number concentration of small CCN-sized particles (> 40 nm in diameter) in the boundary layer with different simulation pairs using a chemical transport model combined with an aerosol microphysics module, GEOS-Chem-TOMAS. Acronyms used for the simulations are adapted from **Paper V**.

Simulation pair	MEAN ΔN40 (%)	MAX |ΔN40| (%)
1. SURF-BASE vs. MASS-BASE	10.8	> 100 [a]
2. SURF-XSOA vs. SURF-BASE	13.7	> 100 [b]
3. SURF-XSOA-H vs. SURF-XSOA	-1.0	10 [b]
4. SURF-XSOA-K vs. SURF-XSOA	-0.03	< 1

[a] Over biogenically active areas (continental tropics). [b] Over anthropogenic source regions.

Significant increase of around 14% in the number concentrations of CCN-sized particles was observed when extra-SOA was applied to the kinetic simulation compared to the case where only traditional BSOA was accounted for. In anthropogenically active areas, e.g. Western North America and Western Europe, the increase was even higher, exceeding 50%. However, with the high additional organic mass load, even 70% decreases in concentrations of small (< 10 nm) particles were obtained. Even though extra-SOA is associated with enhanced nanoparticle growth, it also increases the coagulation sink for freshly nucleated particles. Also, when more sulfuric acid, among organic matter, condenses onto larger particles nucleation potential is suppressed. Thus, with extra-SOA in the model, simulated particle size distributions matched better with the measured ones – less particles in the nucleation mode and more in the CCN-sizes. To note, uncertainties in the other aerosol

dynamic processes, e.g. nucleation, dry deposition and emissions of primary aerosols, cause uncertainty to the simulated aerosol size distributions and hence, to the estimation of CCN-sized particle numbers (Lee et al., 2013).

Parameterization of sub-20 nm particle growth was implemented in the model with a kinetic scheme and extra-SOA. The semi-empirical scaling factors obtained using the European data set for traditional BSOA were used for all SOA, for simplicity (**Paper V**). The parameterization resulted in a global decrease of 4-6% in sub-10 nm particle concentrations, even exceeding 50% on a regional scale, due to suppressed particle growth leading to increase in coagulational scavenging of these small particles. Global decrease of 1% in N40 was observed. This decrease is within the uncertainties associated with the model and hence, cannot be considered significant. Regionally the decrease in the number concentration of CCN-sized particles was up to 10%. Growth parameterization of sub-3 nm particles had insignificant effect on particle numbers – even the decreases in sub-10 nm particle concentrations were less than 1%. These results indicate that the overall SOA production is a larger source of uncertainty in CCN numbers than the size-dependency of the growth.

5 Review of papers and the author's contribution

This thesis contains five papers. I am solely responsible for the introduction of this thesis.

Paper I reports long-term analysis of field measurements on aerosol volatility in a boreal forest site in Hyytiälä, Finland. To understand the observed aerosol volatility and its seasonal behavior, additional independent data sets, e.g. of black carbon and aerosol chemical composition, were applied to the analysis. Significant amount of effectively non-volatile (not evaporating at 280 ˚C) aerosol material was found in submicron particles. Part of this non-volatile residual mass was explained by black carbon. The rest of the non-volatile residual was related to both biogenic and anthropogenic compounds, likely organics. I performed the data analysis and wrote most of the paper.

Paper II investigates the effect of monovalent inorganic salts (sodium chloride and ammonium sulfate) on the volatility of weak organic acids (acetic, oxalic, succinic and citric acid) by combining laboratory experiments using TPD aerosol-CIMS with a process model of aerosol evaporation. Inorganic salts were observed to lower the volatility of organic acids with low-enough pure-component volatility. The modeled organic acid evaporation from the dried aerosol mixtures matched with the experimental results only when a fraction of the initial organic acid amount was assumed to be converted to effectively non-volatile organic material upon drying. I did the experimental work and model analysis, and wrote most of the article.

In **Paper III** organic acid-inorganic salt interactions and their effect on aerosol volatility and hygroscopicity were investigated. Oxalic acid was chosen to represent atmospherically relevant dicarboxylic acid and it was mixed with both monovalent and divalent inorganic salts, sodium chloride and several metal chloride salts, respectively. The results on aerosol volatility suggested enhanced partitioning of oxalic acid due to oxalate formation. Addition of oxalic acid to divalent salt aerosol lead to formation of particles with very low hygroscopicity, likely due to formation of insoluble metal-oxalate particle coating. With sodium salt dominated particles, similar effect on particle hygroscopicity was not observed. I did the experimental work and data analysis related to the TPD aerosol-CIMS and aerosol volatility, and contributed to writing the article.

Paper IV introduces a semi-empirical size-dependent parameterization of sub-20 nm particle growth developed for the purposes of large-scale atmospheric models. It was assumed that nanoparticle growth can be explained solely by condensation of sulfuric acid, first-order products from monoterpene oxidation and some additional organic material (extra-SOA precursor). Distribution of the organic material onto the nanoparticles according to their size – 1.5-3 nm, 3-7 nm and 7-20 nm – was done by using scaling factors. The parameters (scaling factors and the amount of extra-SOA) were determined empirically using long-term particle growth rate data and other relevant data from Hyytiälä and five other continental European sites. The parameterization was able to capture the observed size-dependent growth of nanoparticles well on a seasonal scale. Extra-SOA precursors

were related to biogenic organic matter formed under anthropogenic influence. In this paper, I did most part of the data analysis and modeling, and wrote most of the article.

Paper V investigates the sensitivity of simulated number concentrations of CCN-sized particles to organic condensation, including the size-dependent parameterization developed in **Paper IV** in an atmospheric model. The size-dependency of the nanoparticle growth did not have a significant effect on global number concentrations of CCN-sized particles but sub-20 nm particle numbers were affected notably on a regional scale. In this paper, I advised in applying the size-dependent sub-20 nm particle growth parameterization (**Paper IV**) to global aerosol microphysics model and contributed to writing the article.

6 Conclusions

Knowing the amount, formation mechanisms and properties of atmospheric secondary organics is crucial for predicting the number concentrations of CCN-sized particles and their climate impacts. This thesis concludes that the interactions between natural and anthropogenic atmospheric compounds can enhance the formation of secondary organic aerosol leading to formation of organic material of low-volatility. The low-volatility material is of special importance when nanoparticles are growing in the atmosphere eventually reaching climate-relevant sizes. An overview of the results and methods used in this thesis and the global relevance of the presented work are illustrated in Fig. 9. Below, answers to the research questions Q1-Q3 defined in Sect. 1 will be given and future directions are discussed.

1) *Effectively non-volatile organic compounds exist in submicron atmospheric aerosol in a boreal forest environment.* The findings of **Paper I** suggest that the fraction of the non-volatile aerosol residual, not consisting of black carbon, is related to organics, both biogenic and anthropogenic in origin. Biogenic organics, possibly organic nitrogen-containing compounds including aminium salts and organonitrates, may contribute significantly to the non-volatile aerosol residual. In addition, especially during winter, non-volatile anthropogenic organic compounds emitted from local combustion processes are likely to play an important role. The results indicate that the organic aerosol in areas with high biogenic activity is not solely natural but human activity can notably affect the aerosol chemical composition and thus, volatility. Therefore, the presence of effectively non-volatile secondary biogenic organic aerosol formed under anthropogenic influence should also be considered. In the future, measurements with high-resolution aerosol mass spectrometer (as in Huffman et al., 2009a; Huffman et al., 2009b) can shed light into the actual composition of the observed non-volatile aerosol residual in the boreal forest and the observed seasonal changes in it.

2) *Organic salt formation within organic acid-inorganic salt mixtures modifies aerosol volatility and hygroscopicity.* The results in **Papers II** and **III** show that interactions between organic and inorganic aerosol constituents can effectively modify aerosol chemical properties and further affect the CCN activity of the particles in both natural and anthropogenically influenced areas. Organic salt formation was observed to lead to less volatile particles in organic acid-inorganic salt aerosol upon drying. Depending on the inorganic salt, particle hygroscopicity was observed to either drop (divalent inorganic salt mixtures) or remain similar (monovalent inorganic salt mixtures) when small amount of organic acid was added to the inorganic salt aerosol. Significant lowering of the particle hygroscopicity may be related to formation of insoluble organic salt coating suggesting that particle morphology can strongly influence the observed aerosol properties. The studies highlight the importance of understanding the reactions occurring between aerosol organic and inorganic constituents, as well as the

need for taking the reactions into account in atmospheric models that currently treat aerosol organic and inorganic fractions independently. Particulate-phase processing in organic acid-ammonium sulfate mixtures may also provide one plausible explanation for the observed anthropogenic enhancement in the formation of biogenic organic aerosol.

3) *Size-dependent nanoparticle growth is mainly explained by condensation of secondary organic compounds. In addition to monoterpene oxidation products, contribution of biogenic organic material formed under anthropogenic influence is probably important in particle growth and should be accounted for in atmospheric models for more accurate assessment of climate-relevant particle numbers.* With the developed parameterization of sub-20 nm particle growth in **Paper IV**, the observed size-dependency in particle growth was captured well on a seasonal scale using data from six continental European measurement sites. The majority of particle growth was explained by atmospheric organics – oxidation products of monoterpenes and other organic matter referred to as extra-SOA. The extra-SOA was related to anthropogenically controlled organic compounds, e.g. biogenic organics formed under anthropogenic influence. The simplicity and low computational cost ensure that the developed parameterization is easy to apply in atmospheric models. **Paper V** concluded that the size-dependent parameterization of sub-20 nm particle growth does not have a drastic effect on the predicted number concentrations of small CCN-sized particles globally, while regionally the effect may be important. The growth parameterization led to significant global decreases in the modeled number concentrations of sub-10 nm particles but the effect was dampened upon further particle growth in the model due to other microphysical processes. However, accounting for the extra-SOA can significantly increase climate-relevant particle numbers globally.

This thesis supports the previous studies suggesting that anthropogenic pollution is of importance in biogenic organic aerosol formation, by providing evidence from field and laboratory measurements and by assessing its significance in nanoparticle growth and the estimation of climate relevant particle numbers (Fig. 9). However, there are still gaps in the knowledge of the amount and properties of atmospheric condensable organic matter. Even though constraining the global SOA amount may be easier than resolving various aerosol properties, large uncertainties still exist in the estimation of global SOA mass budget. In addition, further studies are needed to improve the mechanistic understanding of the formation of eBSOA, and the influence of the anthropogenic enhancement on the properties of biogenic organic aerosol.

Both gaseous- and particulate-phase formation of low-volatility eBSOA can take place as suggested in **Papers I** and **II**, highlighting the need to quantify the relevance of the formation mechanisms in different environments through e.g. combinations of field campaigns and controlled laboratory experiments. Formation of low-volatility organic salts within laboratory-generated particles was discussed as one possible pathway to form low-

volatility eBSOA via organic acid-inorganic salt interactions (**Paper II**). The contribution of these organic-inorganic reactions for the growth of nanoparticles in atmospheric conditions is left for future studies. Organic salt formation can explain a significant fraction of atmospheric sub-20 nm particle growth but is more likely to involve aminium-organic acid neutralization than ammonium-organic acid reactions (Smith et al., 2010; Riipinen et al., 2012). In the atmosphere, the contribution of ammonium to particle mass typically becomes more significant when particles get larger (> 100 nm) indicating that organic acid-ammonium sulfate interactions may be important in these sizes.

Eventually, the increased understanding will lead to process parameterization of organic aerosol formation under different conditions accounting for the influence of human activity. These parameterizations are needed to improve separation between anthropogenic and natural organic aerosol in atmospheric models for more accurate predictions on the effect of anthropogenically controlled organic aerosol on climate change. If accounted for, eBSOA will certainly affect the predictions of organic aerosol climate effects (**Paper V**; Spracklen et al., 2011). In addition, the fact that a notable fraction of SOA is controllable – larger fraction than previously thought – is expected to lead to more effective air quality regulations and management in the future (Carlton et al., 2010).

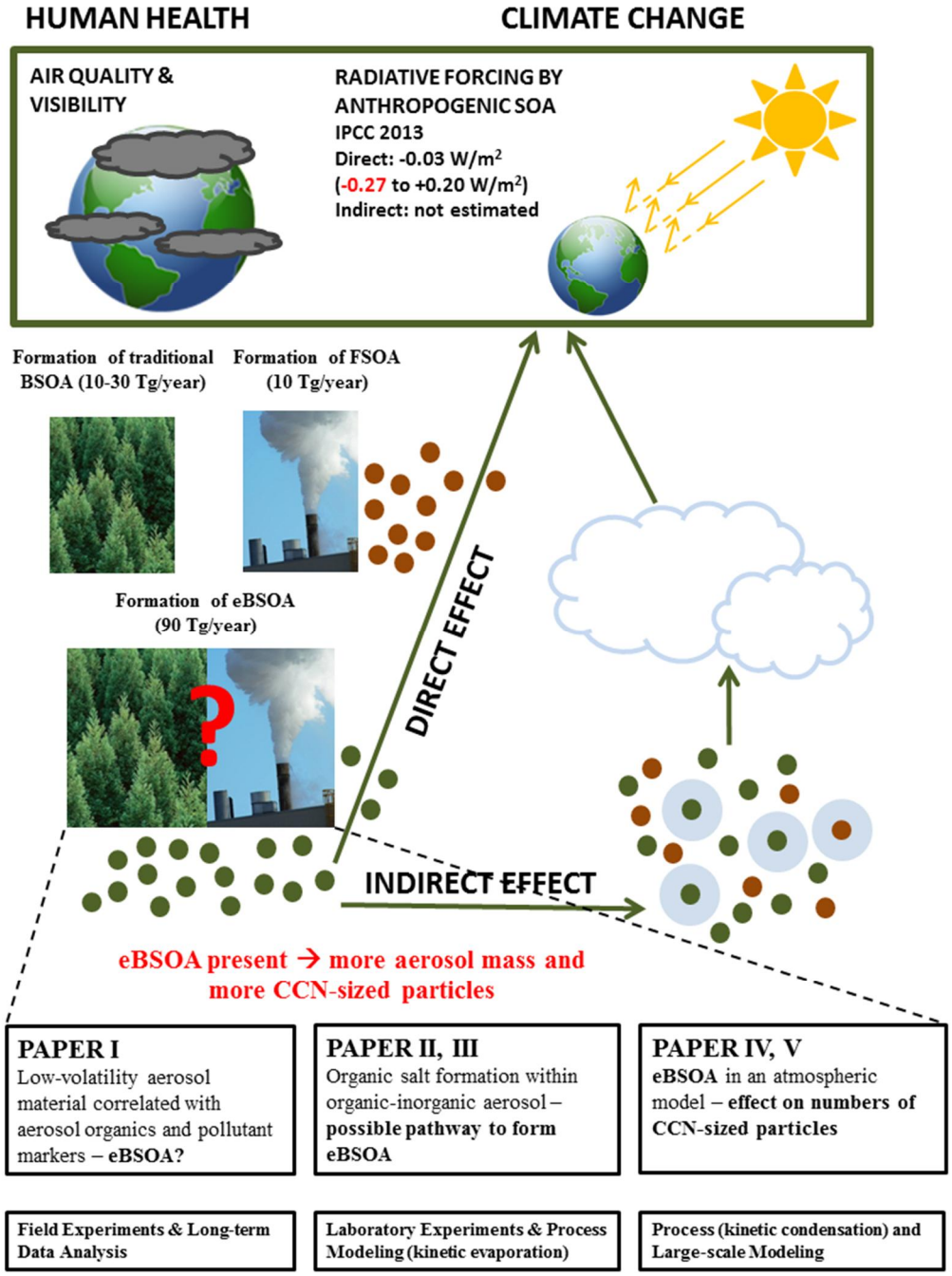

Figure 9: A schematic bringing together all the main results of the thesis – formation of biogenic secondary organic aerosol under anthropogenic influence (eBSOA) and its importance in predicting the effect of organic aerosol on climate change. Radiative forcing (direct effect) of ASOA is likely to be in the lower range of values proposed by IPCC (2013) since mass loadings of ASOA are currently underestimated in many IPCC models (Spracklen et al., 2011; Tsigaridis et al., 2014). Presented SOA source strengths are from Spracklen et al. (2011).

References

Aalto, P., Hämeri, K., Becker, E. D. O., Weber, R., Salm, J., Mäkelä, J. M., Hoell, C., O'Dowd, C. D., Karlsson, H., Hansson, H.-C., Väkevä, M., Koponen, I. K., Buzorius, G., and Kulmala, M. (2001). Physical characterization of aerosol particles during nucleation events. *Tellus B*, 53(4): 344-358.

An, W. J., Pathak, R. K., Lee, B.-H., and Pandis, S. N. (2007). Aerosol volatility measurement using an improved thermodenuder: Application to secondary organic aerosol. *J. Aerosol Sci.*, 38(3): 305-314.

Backman, J., Virkkula, A., Petäjä, T., Aurela, M., Frey, A., and Hillamo, R. (2010). Impacts of volatilisation on light scattering and filter-based absorption measurements: a case study. *Atmos. Meas. Tech.*, 3(5): 1205-1216.

Barsanti, K. C., McMurry, P. H., and Smith, J. N. (2009). The potential contribution of organic salts to new particle growth. *Atmos. Chem. Phys.*, 9(9): 2949-2957.

Bilde, M., Svenningsson, B., Mønster, J., and Rosenørn, T. (2003). Even-odd alternation of evaporation rates and vapor pressures of C3-C9 dicarboxylic acid aerosols. *Environ. Sci. Technol.*, 37(7): 1371-1378.

Bilde, M., Barsanti, K., Booth, M., Cappa, C. D., Donahue, N. M., Emanuelsson, E. U., McFiggans, G., Krieger, U. K., Marcolli, C., Topping, D., Ziemann, P., Barley, M., Clegg, S., Dennis-Smither, B., Hallquist, M., Hallquist, Å. M., Khlystov, A., Kulmala, M., Mogensen, D., Percival, C. J., Pope, F., Reid, J. P., Ribeiro da Silva, M. A. V., Rosenoern, T., Salo, K., Soonsin, V. P., Yli-Juuti, T., Prisle, N. L., Pagels, J., Rarey, J., Zardini, A. A., and Riipinen, I. (2015). Saturation vapor pressures and transition enthalpies of low-volatility organic molecules of atmospheric relevance: From dicarboxylic acids to complex mixtures. *Chem. Rev.*, DOI: 10.1021/cr5005502.

Birmili, W., Heinke, K., Pitz, M., Matschullat, J., Wiedensohler, A., Cyrys, J., Wichmann, H. E., and Peters, A. (2010). Particle number size distributions in urban air before and after volatilisation. *Atmos. Chem. Phys.*, 10(10): 4643-4660.

Booth, A. M., Markus, T., McFiggans, G., Percival, C. J., Mcgillen, M. R., and Topping, D. O. (2009). Design and construction of a simple Knudsen Effusion Mass Spectrometer (KEMS) system for vapour pressure measurements of low volatility organics. *Atmos. Meas. Tech.*, 2(2): 355-361.

Cabada, J. C., Khlystov, A., Wittig, A. E., Pilinis, C., and Pandis, S. N. (2004). Light scattering by fine particles during the Pittsburgh Air Quality Study: Measurements and modeling. *J. Geophys. Res.*, 109: D16S03.

Cappa, C. D., Lovejoy, E. R., and Ravishankara, A. R. (2007). Determination of evaporation rates and vapor pressures of very low volatility compounds: A study of the C4-C10 and C12 dicarboxylic acids. *J. Phys. Chem. A*, 111(16): 3099-3109.

Carlton, A. G., Pinder, R. W., Bhave, P. V., and Pouliot, G. A. (2010). To what extent can biogenic SOA be controlled? *Environ. Sci. Technol.*, 44(9): 3376-3380.

Carlton, A. G. and Turpin, B. J. (2013). Particle partitioning potential of organic compounds is highest in the Eastern US and driven by anthropogenic water. *Atmos. Chem. Phys.*, 13(20): 10203-10214.

Chattopadhyay, S. and Ziemann, P. J. (2005). Vapor pressures of substituted and unsubstituted monocarboxylic and dicarboxylic acids measured using an improved thermal desorption particle beam mass spectrometry method. *Aerosol Sci. Technol.*, 39(11): 1085-1100.

Clegg, S. L. and Seinfeld, J. H. (2006a). Thermodynamic models of aqueous solutions containing inorganic electrolytes and dicarboxylic acids at 298.15 K. 2. Systems including dissociation equilibria. *J. Phys. Chem. A*, 110(17): 5718-5734.

Clegg, S. L. and Seinfeld, J. H. (2006b). Thermodynamic models of aqueous solutions containing inorganic electrolytes and dicarboxylic acids at 298.15 K. 1. The acids as nondissociating components. *J. Phys. Chem. A*, 110(17): 5692-5717.

Dal Maso, M., Kulmala, M., Riipinen, I., Wagner, R., Hussein, T., Aalto, P. P., and Lehtinen, K. E. J. (2005). Formation and growth of fresh atmospheric aerosols: Eight years of aerosol size distribution data from SMEAR II, Hyytiälä, Finland. *Boreal Environ. Res.*, 10(5): 323-336.

Davidson, C. I., Phalen, R. F., and Solomon, P. A. (2005). Airborne particulate matter and human health: a review. *Aerosol Sci. Technol.*, 39(8): 737-749.

De Gouw, J. and Jimenez, J. L. (2009). Organic aerosols in the Earth's atmosphere. *Environ. Sci. Technol.*, 43(20): 7614-7618.

Dinar, E., Anttila, T., and Rudich, Y. (2008). CCN activity and hygroscopic growth of organic aerosols following reactive uptake of ammonia. *Environ. Sci. Technol.*, 42(3): 793-799.

Dockery, D. W., Pope, C. A., Xu, X., Spengler, J. D., Ware, J. H., Fay, M. E., Ferris Jr, B. G., and Speizer, F. E. (1993). An association between air pollution and mortality in six US cities. *N. Engl. J. Med.*, 329(24): 1753-1759.

Donahue, N. M., Robinson, A. L., Stanier, C. O., and Pandis, S. N. (2006). Coupled partitioning, dilution, and chemical aging of semivolatile organics. *Environ. Sci. Technol.*, 40(8): 2635-2643.

Donahue, N. M., Ortega, I. K., Chuang, W., Riipinen, I., Riccobono, F., Schobesberger, S., Dommen, J., Baltensperger, U., Kulmala, M., Worsnop, D. R., and Vehkamaki, H. (2013). How do organic vapors contribute to new-particle formation? *Faraday Discuss.*, 165: 91-104.

Dusek, U., Frank, G. P., Hildebrandt, L., Curtius, J., Schneider, J., Walter, S., Chand, D., Drewnick, F., Hings, S., Jung, D., Borrmann, S., and Andreae, M. O. (2006). Size matters more than chemistry for cloud-nucleating ability of aerosol particles. *Science*, 312(5778): 1375-1378.

Ehn, M., Petäjä, T., Birmili, W., Junninen, H., Aalto, P., and Kulmala, M. (2007). Non-volatile residuals of newly formed atmospheric particles in the boreal forest. *Atmos. Chem. Phys.*, 7(3): 677-684.

Ehn, M., Thornton, J. A., Kleist, E., Sipila, M., Junninen, H., Pullinen, I., Springer, M., Rubach, F., Tillmann, R., Lee, B., Lopez-Hilfiker, F., Andres, S., Acir, I. H., Rissanen, M., Jokinen, T., Schobesberger, S., Kangasluoma, J., Kontkanen, J., Nieminen, T., Kurten, T., Nielsen, L. B., Jorgensen, S., Kjaergaard, H. G., Canagaratna, M., Maso, M. D., Berndt, T., Petaja, T., Wahner, A., Kerminen, V. M., Kulmala, M., Worsnop, D. R., Wildt, J., and

Mentel, T. F. (2014). A large source of low-volatility secondary organic aerosol. *Nature*, 506(7489): 476-479.

Ervens, B., Turpin, B. J., and Weber, R. J. (2011). Secondary organic aerosol formation in cloud droplets and aqueous particles (aqSOA): a review of laboratory, field and model studies. *Atmos. Chem. Phys.*, 11(21): 11069-11102.

Farina, S. C., Adams, P. J., and Pandis, S. N. (2010). Modeling global secondary organic aerosol formation and processing with the volatility basis set: Implications for anthropogenic secondary organic aerosol. *J. Geophys. Res.*, 115: D09202.

Fry, J. L., Kiendler-Scharr, A., Rollins, A. W., Wooldridge, P. J., Brown, S. S., Fuchs, H., Dubé, W., Mensah, A., dal Maso, M., Tillmann, R., Dorn, H. P., Brauers, T., and Cohen, R. C. (2009). Organic nitrate and secondary organic aerosol yield from NO3 oxidation of β-pinene evaluated using a gas-phase kinetics/aerosol partitioning model. *Atmos. Chem. Phys.*, 9(4): 1431-1449.

Fu, P., Kawamura, K., Usukura, K., and Miura, K. (2013). Dicarboxylic acids, ketocarboxylic acids and glyoxal in the marine aerosols collected during a round-the-world cruise. *Mar. Chem.*, 148: 22-32.

Fuchs, N. A. and Sutugin, A. G. (1970). *Highly Dispersed Aerosols*. Ann Arbor Science Publisher, Ann Arbor, USA.

Gao, S., Ng, N. L., Keywood, M., Varutbangkul, V., Bahreini, R., Nenes, A., He, J., Yoo, K. Y., Beauchamp, J. L., Hodyss, R. P., Flagan, R. C., and Seinfeld, J. H. (2004). Particle phase acidity and oligomer formation in secondary organic aerosol. *Environ. Sci. Technol.*, 38(24): 6582-6589.

Goldstein, A. H. and Galbally, I. E. (2007). Known and unexplored organic constituents in the Earth's atmosphere. *Environ. Sci. Technol.*, 41(5): 1514-1521.

Good, N., Topping, D. O., Allan, J. D., Flynn, M., Fuentes, E., Irwin, M., Williams, P. I., Coe, H., and McFiggans, G. (2010). Consistency between parameterisations of aerosol hygroscopicity and CCN activity during the RHaMBLe discovery cruise. *Atmos. Chem. Phys.*, 10(7): 3189-3203.

Hallquist, M., Wenger, J. C., Baltensperger, U., Rudich, Y., Simpson, D., Claeys, M., Dommen, J., Donahue, N. M., George, C., Goldstein, A. H., Hamilton, J. F., Herrmann, H., Hoffmann, T., Iinuma, Y., Jang, M., Jenkin, M. E., Jimenez, J. L., Kiendler-Scharr, A., Maenhaut, W., McFiggans, G., Mentel, T. F., Monod, A., Prévôt, A. S. H., Seinfeld, J. H., Surratt, J. D., Szmigielski, R., and Wildt, J. (2009). The formation, properties and impact of secondary organic aerosol: Current and emerging issues. *Atmos. Chem. Phys.*, 9(14): 5155-5236.

Hansen, A. D. A., Rosen, H., and Novakov, T. (1984). The Aethalometer — an instrument for the real-time measurement of optical absorption by aerosol particles. *Sci. Total Environ.*, 36: 191-196.

Hao, L. Q., Kortelainen, A., Romakkaniemi, S., Portin, H., Jaatinen, A., Leskinen, A., Komppula, M., Miettinen, P., Sueper, D., Pajunoja, A., Smith, J. N., Lehtinen, K. E. J., Worsnop, D. R., Laaksonen, A., and Virtanen, A. (2014). Atmospheric submicron aerosol composition and particulate organic nitrate formation in a boreal forestland–urban mixed region. *Atmos. Chem. Phys.*, 14(24): 13483-13495.

Hari, P. and Kulmala, M. (2005). Station for measuring ecosystem-atmosphere relations. *Boreal Environ. Res.*, 10: 315-322.

Haynes, W. M. (Ed.) (2011). *CRC Handbook of Chemistry and Physics*. 92nd ed., CRC, Boca Raton, Fl, USA.

Heald, C. L., Coe, H., Jimenez, J. L., Weber, R. J., Bahreini, R., Middlebrook, A. M., Russell, L. M., Jolleys, M., Fu, T. M., Allan, J. D., Bower, K. N., Capes, G., Crosier, J., Morgan, W. T., Robinson, N. H., Williams, P. I., Cubison, M. J., DeCarlo, P. F., and Dunlea, E. J. (2011). Exploring the vertical profile of atmospheric organic aerosol: Comparing 17 aircraft field campaigns with a global model. *Atmos. Chem. Phys.*, 11(24): 12673-12696.

Hirsikko, A., Laakso, L., Horrak, U., Aalto, P. P., Kerminen, V., and Kulmala, M. (2005). Annual and size dependent variation of growth rates and ion concentrations in boreal forest. *Boreal Environ. Res.*, 10(5): 357-369.

Holzinger, R., Kasper-Giebl, A., Staudinger, M., Schauer, G., and Röckmann, T. (2010). Analysis of the chemical composition of organic aerosol at the Mt. Sonnblick observatory using a novel high mass resolution thermal-desorption proton-transfer-reaction mass-spectrometer (hr-TD-PTR-MS). *Atmos. Chem. Phys.*, 10(20): 10111-10128.

Hong, J., Häkkinen, S. A. K., Paramonov, M., Äijälä, M., Hakala, J., Nieminen, T., Mikkilä, J., Prisle, N. L., Kulmala, M., Riipinen, I., Bilde, M., Kerminen, V. M., and Petäjä, T. (2014). Hygroscopicity, CCN and volatility properties of submicron atmospheric aerosol in a boreal forest environment during the summer of 2010. *Atmos. Chem. Phys.*, 14(9): 4733-4748.

Hoyle, C. R., Boy, M., Donahue, N. M., Fry, J. L., Glasius, M., Guenther, A., Hallar, A. G., Huff Hartz, K., Petters, M. D., Petäjä, T., Rosenoern, T., and Sullivan, A. P. (2011). A review of the anthropogenic influence on biogenic secondary organic aerosol. *Atmos. Chem. Phys.*, 11(1): 321-343.

Huang, R.-J., Zhang, Y., Bozzetti, C., Ho, K.-F., Cao, J.-J., Han, Y., Daellenbach, K. R., Slowik, J. G., Platt, S. M., Canonaco, F., Zotter, P., Wolf, R., Pieber, S. M., Bruns, E. A., Crippa, M., Ciarelli, G., Piazzalunga, A., Schwikowski, M., Abbaszade, G., Schnelle-Kreis, J., Zimmermann, R., An, Z., Szidat, S., Baltensperger, U., Haddad, I. E., and Prevot, A. S. H. (2014). High secondary aerosol contribution to particulate pollution during haze events in China. *Nature*, 514(7521): 218-222.

Huffman, J. A., Ziemann, P. J., Jayne, J. T., Worsnop, D. R., and Jimenez, J. L. (2008). Development and characterization of a fast-stepping/scanning thermodenuder for chemically-resolved aerosol volatility measurements. *Aerosol Sci. Technol.*, 42(5): 395-407.

Huffman, J. A., Docherty, K. S., Aiken, A. C., Cubison, M. J., Ulbrich, I. M., DeCarlo, P. F., Sueper, D., Jayne, J. T., Worsnop, D. R., Ziemann, P. J., and Jimenez, J. L. (2009a). Chemically-resolved aerosol volatility measurements from two megacity field studies. *Atmos. Chem. Phys.*, 9(18): 7161-7182.

Huffman, J. A., Docherty, K. S., Mohr, C., Cubison, M. J., Ulbrich, I. M., Ziemann, P. J., Onasch, T. B., and Jimenez, J. L. (2009b). Chemically-resolved volatility measurements of organic aerosol from different sources. *Environ. Sci. Technol.*, 43(14): 5351-5357.

IPCC (2013): *Climate Change 2013: The Physical Science Basis. Contribution of Working Group I to the Fifth Assessment Report of the Intergovernmental Panel on Climate Change* [Stocker, T. F., Qin, D., Plattner, G.-K., Tignor, M., Allen, S. K., J., B., Nauels, A., Xia, Y.,

Bex, V. and Midgley, P. M. (eds.)]. Cambridge University Press, Cambridge, United Kingdom and New York, NY, USA.

Jang, M., Czoschke, N. M., Lee, S., and Kamens, R. M. (2002). Heterogeneous atmospheric aerosol production by acid-catalyzed particle-phase reactions. *Science*, 298(5594): 814-817.

Jayne, J. T., Leard, D. C., Zhang, X., Davidovits, P., Smith, K. A., Kolb, C. E., and Worsnop, D. R. (2000). Development of an aerosol mass spectrometer for size and composition analysis of submicron particles. *Aerosol Sci. Technol.*, 33(1-2): 49-70.

Jimenez, J. L., Canagaratna, M. R., Donahue, N. M., Prevot, A. S., Zhang, Q., Kroll, J. H., DeCarlo, P. F., Allan, J. D., Coe, H., Ng, N. L., Aiken, A. C., Docherty, K. S., Ulbrich, I. M., Grieshop, A. P., Robinson, A. L., Duplissy, J., Smith, J. D., Wilson, K. R., Lanz, V. A., Hueglin, C., Sun, Y. L., Tian, J., Laaksonen, A., Raatikainen, T., Rautiainen, J., Vaattovaara, P., Ehn, M., Kulmala, M., Tomlinson, J. M., Collins, D. R., Cubison, M. J., Dunlea, E. J., Huffman, J. A., Onasch, T. B., Alfarra, M. R., Williams, P. I., Bower, K., Kondo, Y., Schneider, J., Drewnick, F., Borrmann, S., Weimer, S., Demerjian, K., Salcedo, D., Cottrell, L., Griffin, R., Takami, A., Miyoshi, T., Hatakeyama, S., Shimono, A., Sun, J. Y., Zhang, Y. M., Dzepina, K., Kimmel, J. R., Sueper, D., Jayne, J. T., Herndon, S. C., Trimborn, A. M., Williams, L. R., Wood, E. C., Middlebrook, A. M., Kolb, C. E., Baltensperger, U., and Worsnop, D. R. (2009). Evolution of organic aerosols in the atmosphere. *Science*, 326(5959): 1525-1529.

Johnson, G. R., Ristovski, Z., and Morawska, L. (2004). Method for measuring the hygroscopic behaviour of lower volatility fractions in an internally mixed aerosol. *J. Aerosol Sci.*, 35(4): 443-455.

Julin, J., Winkler, P. M., Donahue, N. M., Wagner, P. E., and Riipinen, I. (2014). Near-unity mass accommodation coefficient of organic molecules of varying structure. *Environ. Sci. Technol.*, 48(20): 12083-12089.

Kalberer, M., Paulsen, D., Sax, M., Steinbacher, M., Dommen, J., Prevot, A. S., Fisseha, R., Weingartner, E., Frankevich, V., Zenobi, R., and Baltensperger, U. (2004). Identification of polymers as major components of atmospheric organic aerosols. *Science*, 303(5664): 1659-1662.

Kanakidou, M., Seinfeld, J. H., Pandis, S. N., Barnes, I., Dentener, F. J., Facchini, M. C., Van Dingenen, R., Ervens, B., Nenes, A., Nielsen, C. J., Swietlicki, E., Putaud, J. P., Balkanski, Y., Fuzzi, S., Horth, J., Moortgat, G. K., Winterhalter, R., Myhre, C. E. L., Tsigaridis, K., Vignati, E., Stephanou, E. G., and Wilson, J. (2005). Organic aerosol and global climate modelling: a review. *Atmos. Chem. Phys.*, 5(4): 1053-1123.

Kawamura, K., Umemoto, N., Mochida, M., Bertram, T., Howell, S., and Huebert, B. J. (2003). Water-soluble dicarboxylic acids in the tropospheric aerosols collected over east Asia and western North Pacific by ACE-Asia C-130 aircraft. *J. Geophys. Res.*, 108(D23): 8639.

Kerminen, V.-M. and Kulmala, M. (2002). Analytical formulae connecting the “real” and the “apparent” nucleation rate and the nuclei number concentration for atmospheric nucleation events. *J. Aerosol Sci.*, 33(4): 609-622.

Kerminen, V. M., Paramonov, M., Anttila, T., Riipinen, I., Fountoukis, C., Korhonen, H., Asmi, E., Laakso, L., Lihavainen, H., Swietlicki, E., Svenningsson, B., Asmi, A., Pandis, S. N., Kulmala, M., and Petäjä, T. (2012). Cloud condensation nuclei production associated

with atmospheric nucleation: a synthesis based on existing literature and new results. *Atmos. Chem. Phys.*, 12(24): 12037-12059.

Kroll, J. H. and Seinfeld, J. H. (2008). Chemistry of secondary organic aerosol: Formation and evolution of low-volatility organics in the atmosphere. *Atmos. Environ.*, 42(16): 3593-3624.

Kuang, C., Chen, M., Zhao, J., Smith, J., McMurry, P. H., and Wang, J. (2012). Size and time-resolved growth rate measurements of 1 to 5 nm freshly formed atmospheric nuclei. *Atmos. Chem. Phys.*, 12(7): 3573-3589.

Kulmala, M., Vehkamäki, H., Petäjä, T., Dal Maso, M., Lauri, A., Kerminen, V. M., Birmili, W., and McMurry, P. H. (2004). Formation and growth rates of ultrafine atmospheric particles: a review of observations. *J. Aerosol Sci.*, 35(2): 143-176.

Kulmala, M., Kontkanen, J., Junninen, H., Lehtipalo, K., Manninen, H. E., Nieminen, T., Petäjä, T., Sipilä, M., Schobesberger, S., Rantala, P., Franchin, A., Jokinen, T., Järvinen, E., Äijälä, M., Kangasluoma, J., Hakala, J., Aalto, P. P., Paasonen, P., Mikkilä, J., Vanhanen, J., Aalto, J., Hakola, H., Makkonen, U., Ruuskanen, T., Mauldin, R. L., Duplissy, J., Vehkamäki, H., Bäck, J., Kortelainen, A., Riipinen, I., Kurtén, T., Johnston, M. V., Smith, J. N., Ehn, M., Mentel, T. F., Lehtinen, K. E. J., Laaksonen, A., Kerminen, V.-M., and Worsnop, D. R. (2013). Direct Observations of Atmospheric Aerosol Nucleation. *Science*, 339(6122): 943-946.

Laskin, A., Moffet, R. C., Gilles, M. K., Fast, J. D., Zaveri, R. A., Wang, B., Nigge, P., and Shutthanandan, J. (2012). Tropospheric chemistry of internally mixed sea salt and organic particles: Surprising reactivity of NaCl with weak organic acids. *J. Geophys. Res.*, 117: D15302.

Lavi, A., Segre, E., Gomez-Hernandez, M., Zhang, R., and Rudich, Y. (2015). Volatility of atmospherically relevant alkylaminium carboxylate salts. *J. Phys. Chem. A*, DOI: 10.1021/jp507320v.

Lee, B. H., Kostenidou, E., Hildebrandt, L., Riipinen, I., Engelhart, G. J., Mohr, C., DeCarlo, P. F., Mihalopoulos, N., Prevot, A. S. H., Baltensperger, U., and Pandis, S. N. (2010). Measurement of the ambient organic aerosol volatility distribution: Application during the Finokalia Aerosol Measurement Experiment (FAME-2008). *Atmos. Chem. Phys.*, 10(24): 12149-12160.

Lee, L. A., Pringle, K. J., Reddington, C. L., Mann, G. W., Stier, P., Spracklen, D. V., Pierce, J. R., and Carslaw, K. S. (2013). The magnitude and causes of uncertainty in global model simulations of cloud condensation nuclei. *Atmos. Chem. Phys*, 13(17): 8879-8914.

Lehtinen, K. E. J. and Kulmala, M. (2003). A model for particle formation and growth in the atmosphere with molecular resolution in size. *Atmos. Chem. Phys.*, 3(1): 251-257.

Leppä, J., Gagné, S., Laakso, L., Manninen, H. E., Lehtinen, K. E. J., Kulmala, M., and Kerminen, V.-M. (2013). Using measurements of the aerosol charging state in determination of the particle growth rate and the proportion of ion-induced nucleation. *Atmos. Chem. Phys.*, 13(1): 463-486.

Liggio, J., Li, S.-M., and McLaren, R. (2005). Heterogeneous reactions of glyoxal on particulate matter: Identification of acetals and sulfate esters. *Environ. Sci. Technol.*, 39(6): 1532-1541.

Lim, Y. B., Tan, Y., Perri, M. J., Seitzinger, S. P., and Turpin, B. J. (2010). Aqueous chemistry and its role in secondary organic aerosol (SOA) formation. *Atmos. Chem. Phys.*, 10(21): 10521-10539.

Lohmann, U. and Feichter, J. (2005). Global indirect aerosol effects: a review. *Atmos. Chem. Phys.*, 5(3): 715-737.

Lopez-Hilfiker, F. D., Mohr, C., Ehn, M., Rubach, F., Kleist, E., Wildt, J., Mentel, T. F., Lutz, A., Hallquist, M., Worsnop, D., and Thornton, J. A. (2014). A novel method for online analysis of gas and particle composition: description and evaluation of a Filter Inlet for Gases and AEROsols (FIGAERO). *Atmos. Meas. Tech.*, 7(4): 983-1001.

Lopez-Hilfiker, F. D., Mohr, C., Ehn, M., Rubach, F., Kleist, E., Wildt, J., Mentel, T. F., Carrasquillo, A., Daumit, K., Hunter, J., Kroll, J. H., Worsnop, D., and Thornton, J. A. (2015). Phase partitioning and volatility of secondary organic aerosol components formed from alpha-pinene ozonolysis and OH oxidation: the importance of accretion products and other low volatility compounds. *Atmos. Chem. Phys. Discuss.*, 15(4): 4463-4494.

Ma, Q., Ma, J., Liu, C., Lai, C., and He, H. (2013). Laboratory study on the hygroscopic behavior of external and internal C2-C4 dicarboxylic acid-NaCl mixtures. *Environ. Sci. Technol.*, 47(18): 10381-10388.

Makkonen, R., Asmi, A., Kerminen, V.-M., Boy, M., Arneth, A., Guenther, A., and Kulmala, M. (2012). BVOC-aerosol-climate interactions in the global aerosol-climate model ECHAM5. 5-HAM2. *Atmos. Chem. Phys.*, 12(21): 10077-10096.

Makkonen, R., Seland, Ø., Kirkevåg, A., Iversen, T., and Kristjánsson, J. E. (2014). Evaluation of aerosol number concentrations in NorESM with improved nucleation parameterization. *Atmos. Chem. Phys.*, 14(10): 5127-5152.

Manninen, H. E., Nieminen, T., Asmi, E., Gagné, S., Häkkinen, S., Lehtipalo, K., Aalto, P., Vana, M., Mirme, A., Mirme, S., Hõrrak, U., Plass-Dülmer, C., Stange, G., Kiss, G., Hoffer, A., Törő, N., Moerman, M., Henzing, B., de Leeuw, G., Brinkenberg, M., Kouvarakis, G. N., Bougiatioti, A., Mihalopoulos, N., O'Dowd, C., Ceburnis, D., Arneth, A., Svenningsson, B., Swietlicki, E., Tarozzi, L., Decesari, S., Facchini, M. C., Birmili, W., Sonntag, A., Wiedensohler, A., Boulon, J., Sellegri, K., Laj, P., Gysel, M., Bukowiecki, N., Weingartner, E., Wehrle, G., Laaksonen, A., Hamed, A., Joutsensaari, J., Petäjä, T., Kerminen, V. M., and Kulmala, M. (2010). EUCAARI ion spectrometer measurements at 12 European sites – analysis of new particle formation events. *Atmos. Chem. Phys.*, 10(16): 7907-7927.

Mauderly, J. L. and Chow, J. C. (2008). Health effects of organic aerosols. *Inhal. Toxicol.*, 20(3): 257-288.

McNeill, V. F., Wolfe, G. M., and Thornton, J. A. (2007). The oxidation of oleate in submicron aqueous salt aerosols: Evidence of a surface process. *J. Phys. Chem. A*, 111(6): 1073-1083.

Merikanto, J., Spracklen, D. V., Mann, G. W., Pickering, S. J., and Carslaw, K. S. (2009). Impact of nucleation on global CCN. *Atmos. Chem. Phys.*, 9(21): 8601-8616.

Murphy, B. N., Donahue, N. M., Robinson, A. L., and Pandis, S. N. (2014). A naming convention for atmospheric organic aerosol. *Atmos. Chem. Phys.*, 14(11): 5825-5839.

Myhre, G., Samset, B. H., Schulz, M., Balkanski, Y., Bauer, S., Berntsen, T. K., Bian, H., Bellouin, N., Chin, M., Diehl, T., Easter, R. C., Feichter, J., Ghan, S. J., Hauglustaine, D., Iversen, T., Kinne, S., Kirkevåg, A., Lamarque, J. F., Lin, G., Liu, X., Lund, M. T., Luo, G.,

Ma, X., van Noije, T., Penner, J. E., Rasch, P. J., Ruiz, A., Seland, Ø., Skeie, R. B., Stier, P., Takemura, T., Tsigaridis, K., Wang, P., Wang, Z., Xu, L., Yu, H., Yu, F., Yoon, J. H., Zhang, K., Zhang, H., and Zhou, C. (2013). Radiative forcing of the direct aerosol effect from AeroCom Phase II simulations. *Atmos. Chem. Phys.*, 13(4): 1853-1877.

Narukawa, M., Kawamura, K., Anlauf, K. G., and Barrie, L. A. (2003). Fine and coarse modes of dicarboxylic acids in the Arctic aerosols collected during the Polar Sunrise Experiment 1997. *J. Geophys. Res.*, 108(D18): 4575.

Nel, A. (2005). Air pollution-related illness: Effects of particles. *Science*, 308(5723): 804-806.

Neusüss, C., Pelzing, M., Plewka, A., and Herrmann, H. (2000). A new analytical approach for size-resolved speciation of organic compounds in atmospheric aerosol particles: Methods and first results. *J. Geophys. Res.*, 105(D4): 4513.

Nguyen, T. B., Lee, P. B., Updyke, K. M., Bones, D. L., Laskin, J., Laskin, A., and Nizkorodov, S. A. (2012). Formation of nitrogen-and sulfur-containing light-absorbing compounds accelerated by evaporation of water from secondary organic aerosols. *J. Geophys. Res.*, 117: D01207.

O'Dowd, C. D., Lowe, J. A., Smith, M. H., Davison, B., Hewitt, C. N., and Harrison, R. M. (1997). Biogenic sulphur emissions and inferred non-sea-salt-sulphate cloud condensation nuclei in and around Antarctica. *J. Geophys. Res.*, 102(D11): 12839-12854.

Ortiz-Montalvo, D. L., Häkkinen, S. A. K., Schwier, A. N., Lim, Y. B., McNeill, V. F., and Turpin, B. J. (2014). Ammonium addition (and aerosol pH) has a dramatic impact on the volatility and yield of glyoxal secondary organic aerosol. *Environ. Sci. Technol.*, 48(1): 255-262.

Paciga, A. L., Riipinen, I., and Pandis, S. N. (2014). Effect of ammonia on the volatility of organic diacids. *Environ. Sci. Technol.*, 48(23): 13769-13775.

Peng, C. and Chan, C. K. (2001). The water cycles of water-soluble organic salts of atmospheric importance. *Atmos. Environ.*, 35(7): 1183-1192.

Philippin, S., Wiedensohler, A., and Stratmann, F. (2004). Measurements of non-volatile fractions of pollution aerosols with an eight-tube volatility tandem differential mobility analyzer (VTDMA-8). *J. Aerosol Sci.*, 35(2): 185-203.

Pierce, J. R. and Adams, P. J. (2009). Uncertainty in global CCN concentrations from uncertain aerosol nucleation and primary emission rates. *Atmos. Chem. Phys.*, 9(4): 1339-1356.

Pierce, J. R., Riipinen, I., Kulmala, M., Ehn, M., Petäjä, T., Junninen, H., Worsnop, D. R., and Donahue, N. M. (2011). Quantification of the volatility of secondary organic compounds in ultrafine particles during nucleation events. *Atmos. Chem. Phys.*, 11(17): 9019-9036.

Pierce, J. R., Evans, M. J., Scott, C. E., D'Andrea, S. D., Farmer, D. K., Swietlicki, E., and Spracklen, D. V. (2013). Weak global sensitivity of cloud condensation nuclei and the aerosol indirect effect to Criegee+ SO2 chemistry. *Atmos. Chem. Phys.*, 13(6): 3163-3176.

Ramanathan, V., Crutzen, P., Kiehl, J., and Rosenfeld, D. (2001). Aerosols, climate, and the hydrological cycle. *Science*, 294(5549): 2119-2124.

Riipinen, I., Pierce, J. R., Donahue, N. M., and Pandis, S. N. (2010). Equilibration time scales of organic aerosol inside thermodenuders: Evaporation kinetics versus thermodynamics. *Atmos. Environ.*, 44(5): 597-607.

Riipinen, I., Pierce, J. R., Yli-Juuti, T., Nieminen, T., Häkkinen, S., Ehn, M., Junninen, H., Lehtipalo, K., Petäjä, T., Slowik, J., Chang, R., Shantz, N. C., Abbatt, J., Leaitch, W. R., Kerminen, V. M., Worsnop, D. R., Pandis, S. N., Donahue, N. M., and Kulmala, M. (2011). Organic condensation: a vital link connecting aerosol formation to cloud condensation nuclei (CCN) concentrations. *Atmos. Chem. Phys.*, 11(8): 3865-3878.

Riipinen, I., Yli-Juuti, T., Pierce, J. R., Petäjä, T., Worsnop, D. R., Kulmala, M., and Donahue, N. M. (2012). The contribution of organics to atmospheric nanoparticle growth. *Nat. Geosci.*, 5(7): 453-458.

Saarikoski, S., Mäkela, T., Hillamo, R., Aalto, P. P., Kerminen, V., and Kulmala, M. (2005). Physico-chemical characterization and mass closure of size-segregated atmospheric aerosols in Hyytiälä, Finland. *Boreal Environ. Res.*, 10(5): 385-400.

Saleh, R., Walker, J., and Khlystov, A. (2008). Determination of saturation pressure and enthalpy of vaporization of semi-volatile aerosols: The integrated volume method. *J. Aerosol Sci.*, 39(10): 876-887.

Saleh, R., Shihadeh, A., and Khlystov, A. (2009). Determination of evaporation coefficients of semi-volatile organic aerosols using an integrated volume—tandem differential mobility analysis (IV-TDMA) method. *J. Aerosol Sci.*, 40(12): 1019-1029.

Saleh, R., Khlystov, A., and Shihadeh, A. (2010). Effect of aerosol generation method on measured saturation pressure and enthalpy of vaporization for dicarboxylic acid aerosols. *Aerosol Sci. Technol.*, 44(4): 302-307.

Salorinne, K., Lahtinen, T., Malola, S., Koivisto, J., and Häkkinen, H. (2014). Solvation chemistry of water-soluble thiol-protected gold nanocluster Au102 from DOSY NMR spectroscopy and DFT calculations. *Nanoscale*, 6(14): 7823-7826.

Sareen, N., Schwier, A. N., Shapiro, E. L., Mitroo, D., and McNeill, V. F. (2010). Secondary organic material formed by methylglyoxal in aqueous aerosol mimics. *Atmos. Chem. Phys.*, 10(3): 997-1016.

Saxena, P. and Hildemann, L. M. (1996). Water-soluble organics in atmospheric particles: a critical review of the literature and application of thermodynamics to identify candidate compounds. *J. Atmos. Chem.*, 24(1): 57-109.

Schulz, M., Textor, C., Kinne, S., Balkanski, Y., Bauer, S., Berntsen, T., Berglen, T., Boucher, O., Dentener, F., Guibert, S., Isaksen, I. S. A., Iversen, T., Koch, D., Kirkevåg, A., Liu, X., Montanaro, V., Myhre, G., Penner, J. E., Pitari, G., Reddy, S., Seland, Ø., Stier, P., and Takemura, T. (2006). Radiative forcing by aerosols as derived from the AeroCom present-day and pre-industrial simulations. *Atmos. Chem. Phys.*, 6(12): 5225-5246.

Schwier, A. N., Sareen, N., Lathem, T. L., Nenes, A., and McNeill, V. F. (2011). Ozone oxidation of oleic acid surface films decreases aerosol cloud condensation nuclei activity. *J. Geophys. Res.*, 116: D16202.

Seinfeld, J. H. and Pandis, S. N. (2006). *Atmospheric Chemistry and Physics: From Air Pollution to Climate Change*. John Wiley & Sons, New Jersey, USA.

Sipilä, M., Berndt, T., Petäjä, T., Brus, D., Vanhanen, J., Stratmann, F., Patokoski, J., Mauldin, R. L., 3rd, Hyvärinen, A. P., Lihavainen, H., and Kulmala, M. (2010). The role of sulfuric acid in atmospheric nucleation. *Science*, 327(5970): 1243-1246.

Smith, J. N., Barsanti, K. C., Friedli, H. R., Ehn, M., Kulmala, M., Collins, D. R., Scheckman, J. H., Williams, B. J., and McMurry, P. H. (2010). Observations of aminium salts in atmospheric nanoparticles and possible climatic implications. *Proc. Nat. Acad. Sci.*, 107(15): 6634-6639.

Soonsin, V., Zardini, A. A., Marcolli, C., Zuend, A., and Krieger, U. K. (2010). The vapor pressures and activities of dicarboxylic acids reconsidered: the impact of the physical state of the aerosol. *Atmos. Chem. Phys.*, 10(23): 11753-11767.

Spracklen, D. V., Pringle, K. J., Carslaw, K. S., Chipperfield, M. P., and Mann, G. W. (2005a). A global off-line model of size-resolved aerosol microphysics: I. Model development and prediction of aerosol properties. *Atmos. Chem. Phys.*, 5(8): 2227-2252.

Spracklen, D. V., Pringle, K. J., Carslaw, K. S., Chipperfield, M. P., and Mann, G. W. (2005b). A global off-line model of size-resolved aerosol microphysics: II. Identification of key uncertainties. *Atmos. Chem. Phys.*, 5(12): 3233-3250.

Spracklen, D. V., Jimenez, J. L., Carslaw, K. S., Worsnop, D. R., Evans, M. J., Mann, G. W., Zhang, Q., Canagaratna, M. R., Allan, J., Coe, H., McFiggans, G., Rap, A., and Forster, P. (2011). Aerosol mass spectrometer constraint on the global secondary organic aerosol budget. *Atmos. Chem. Phys.*, 11(23): 12109-12136.

Stier, P., Seinfeld, J. H., Kinne, S., and Boucher, O. (2007). Aerosol absorption and radiative forcing. *Atmos. Chem. Phys.*, 7(19): 5237-5261.

Stolzenburg, M. R., McMurry, P. H., Sakurai, H., Smith, J. N., Mauldin, R. L., Eisele, F. L., and Clement, C. F. (2005). Growth rates of freshly nucleated atmospheric particles in Atlanta. *J. Geophys. Res.*, 110: D22S05.

Surratt, J. D., Kroll, J. H., Kleindienst, T. E., Edney, E. O., Claeys, M., Sorooshian, A., Ng, N. L., Offenberg, J. H., Lewandowski, M., Jaoui, M., Flagan, R. C., and Seinfeld, J. H. (2007). Evidence for organosulfates in secondary organic aerosol. *Environ. Sci. Technol.*, 41(2): 517-527.

Topping, D. O., McFiggans, G. B., Kiss, G., Varga, Z., Facchini, M. C., Decesari, S., and Mircea, M. (2007). Surface tensions of multi-component mixed inorganic/organic aqueous systems of atmospheric significance: Measurements, model predictions and importance for cloud activation predictions. *Atmos. Chem. Phys.*, 7(9): 2371-2398.

Tritscher, T., Dommen, J., DeCarlo, P. F., Gysel, M., Barmet, P. B., Praplan, A. P., Weingartner, E., Prévôt, A. S. H., Riipinen, I., Donahue, N. M., and Baltensperger, U. (2011). Volatility and hygroscopicity of aging secondary organic aerosol in a smog chamber. *Atmos. Chem. Phys.*, 11(22): 11477-11496.

Tsigaridis, K., Daskalakis, N., Kanakidou, M., Adams, P. J., Artaxo, P., Bahadur, R., Balkanski, Y., Bauer, S. E., Bellouin, N., Benedetti, A., Bergman, T., Berntsen, T. K., Beukes, J. P., Bian, H., Carslaw, K. S., Chin, M., Curci, G., Diehl, T., Easter, R. C., Ghan, S. J., Gong, S. L., Hodzic, A., Hoyle, C. R., Iversen, T., Jathar, S., Jimenez, J. L., Kaiser, J. W., Kirkevåg, A., Koch, D., Kokkola, H., Lee, Y. H., Lin, G., Liu, X., Luo, G., Ma, X., Mann, G. W., Mihalopoulos, N., Morcrette, J. J., Müller, J. F., Myhre, G., Myriokefalitakis, S., Ng, N. L., O'Donnell, D., Penner, J. E., Pozzoli, L., Pringle, K. J., Russell, L. M., Schulz,

M., Sciare, J., Seland, Ø., Shindell, D. T., Sillman, S., Skeie, R. B., Spracklen, D., Stavrakou, T., Steenrod, S. D., Takemura, T., Tiitta, P., Tilmes, S., Tost, H., van Noije, T., van Zyl, P. G., von Salzen, K., Yu, F., Wang, Z., Wang, Z., Zaveri, R. A., Zhang, H., Zhang, K., Zhang, Q., and Zhang, X. (2014). The AeroCom evaluation and intercomparison of organic aerosol in global models. *Atmos. Chem. Phys.*, 14(19): 10845-10895.

Weber, R. J., Marti, J. J., McMurry, P. H., Eisele, F. L., Tanner, D. J., and Jefferson, A. (1997). Measurements of new particle formation and ultrafine particle growth rates at a clean continental site. *J. Geophys. Res.*, 102(D4): 4375-4385.

Weber, R. J., Sullivan, A. P., Peltier, R. E., Russell, A., Yan, B., Zheng, M., de Gouw, J., Warneke, C., Brock, C., Holloway, J. S., Atlas, E. L., and Edgerton, E. (2007). A study of secondary organic aerosol formation in the anthropogenic-influenced southeastern United States. *J. Geophys. Res.*, 112: D13302.

Vehkamäki, H. and Riipinen, I. (2012). Thermodynamics and kinetics of atmospheric aerosol particle formation and growth. *Chem. Soc. Rev.*, 41(15): 5160-5173.

Wehner, B., Philippin, S., and Wiedensohler, A. (2002). Design and calibration of a thermodenuder with an improved heating unit to measure the size-dependent volatile fraction of aerosol particles. *J. Aerosol Sci.*, 33(7): 1087-1093.

Wehner, B., Philippin, S., Wiedensohler, A., Scheer, V., and Vogt, R. (2004). Variability of non-volatile fractions of atmospheric aerosol particles with traffic influence. *Atmos. Environ.*, 38(36): 6081-6090.

Wehner, B., Petäjä, T., Boy, M., Engler, C., Birmili, W., Tuch, T., Wiedensohler, A., and Kulmala, M. (2005). The contribution of sulfuric acid and non-volatile compounds on the growth of freshly formed atmospheric aerosols. *Geophys. Res. Lett.*, 32: L17810.

Villani, P., Picard, D., Marchand, N., and Laj, P. (2007). Design and Validation of a 6-Volatility Tandem Differential Mobility Analyzer (VTDMA). *Aerosol Sci. Technol.*, 41(10): 898-906.

Williams, B. J., Goldstein, A. H., Kreisberg, N. M., and Hering, S. V. (2006). An In-Situ Instrument for Speciated Organic Composition of Atmospheric Aerosols: Thermal Desorption Aerosol GC/MS-FID (TAG). *Aerosol Sci. Technol.*, 40(8): 627-638.

Winkler, P. M., Vrtala, A., Rudolf, R., Wagner, P. E., Riipinen, I., Vesala, T., Lehtinen, K. E. J., Viisanen, Y., and Kulmala, M. (2006). Condensation of water vapor: Experimental determination of mass and thermal accommodation coefficients. *J. Geophys. Res.*, 111: D19202.

Virtanen, A., Joutsensaari, J., Koop, T., Kannosto, J., Yli-Pirilä, P., Leskinen, J., Mäkela, J. M., Holopainen, J. K., Pöschl, U., Kulmala, M., Worsnop, D. R., and Laaksonen, A. (2010). An amorphous solid state of biogenic secondary organic aerosol particles. *Nature*, 467(7317): 824-827.

Volkamer, R., Jimenez, J. L., San Martini, F., Dzepina, K., Zhang, Q., Salcedo, D., Molina, L. T., Worsnop, D. R., and Molina, M. J. (2006). Secondary organic aerosol formation from anthropogenic air pollution: Rapid and higher than expected. *Geophys. Res. Lett.*, 33: L17811.

Yaws, C. L. (2003). *Yaws' Handbook of Thermodynamic and Physical Properties of Chemical Compounds*. Knovel; http://app.knovel.com/hotlink/toc/id:kpYHTPPCC4/yaws-handbook-thermodynamic/yaws-handbook-thermodynamic (Sep 6th 2014).

Yli-Juuti, T., Riipinen, I., Aalto, P. P., Nieminen, T., Maenhaut, W., Janssens, I. A., Claeys, M., Salma, I., Ocskay, R., Hoffer, A., Imre, K., and Kulmala, M. (2009). Characteristics of new particle formation events and cluster ions at K-puszta, Hungary. *Boreal Environ. Res.*, 14(4): 683-698.

Yli-Juuti, T., Nieminen, T., Hirsikko, A., Aalto, P. P., Asmi, E., Hõrrak, U., Manninen, H. E., Patokoski, J., Dal Maso, M., Petäjä, T., Rinne, J., Kulmala, M., and Riipinen, I. (2011). Growth rates of nucleation mode particles in Hyytiälä during 2003-2009: Variation with particle size, season, data analysis method and ambient conditions. *Atmos. Chem. Phys.*, 11(24): 12865-12886.

Yli-Juuti, T., Barsanti, K., Hildebrandt Ruiz, L., Kieloaho, A. J., Makkonen, U., Petäjä, T., Ruuskanen, T., Kulmala, M., and Riipinen, I. (2013a). Model for acid-base chemistry in nanoparticle growth (MABNAG). *Atmos. Chem. Phys.*, 13(24): 12507-12524.

Yli-Juuti, T., Zardini, A. A., Eriksson, A. C., Hansen, A. M., Pagels, J. H., Swietlicki, E., Svenningsson, B., Glasius, M., Worsnop, D. R., Riipinen, I., and Bilde, M. (2013b). Volatility of organic aerosol: Evaporation of ammonium sulfate/succinic acid aqueous solution droplets. *Environ. Sci. Technol.*, 47(21): 12123-12130.

Yu, H., Ortega, J., Smith, J. N., Guenther, A. B., Kanawade, V. P., You, Y., Liu, Y., Hosman, K., Karl, T., Seco, R., Geron, C., Pallardy, S. G., Gu, L., Mikkilä, J., and Lee, S.-H. (2014). New particle formation and growth in an isoprene-dominated ozark forest: From sub-5 nm to CCN-active sizes. *Aerosol Sci. Technol.*, 48(12): 1285-1298.

Zardini, A. A., Riipinen, I., Koponen, I. K., Kulmala, M., and Bilde, M. (2010). Evaporation of ternary inorganic/organic aqueous droplets: Sodium chloride, succinic acid and water. *J. Aerosol Sci.*, 41(8): 760-770.

Zhang, Q., Jimenez, J. L., Canagaratna, M. R., Allan, J. D., Coe, H., Ulbrich, I., Alfarra, M. R., Takami, A., Middlebrook, A. M., Sun, Y. L., Dzepina, K., Dunlea, E., Docherty, K., DeCarlo, P. F., Salcedo, D., Onasch, T., Jayne, J. T., Miyoshi, T., Shimono, A., Hatakeyama, S., Takegawa, N., Kondo, Y., Schneider, J., Drewnick, F., Borrmann, S., Weimer, S., Demerjian, K., Williams, P., Bower, K., Bahreini, R., Cottrell, L., Griffin, R. J., Rautiainen, J., Sun, J. Y., Zhang, Y. M., and Worsnop, D. R. (2007). Ubiquity and dominance of oxygenated species in organic aerosols in anthropogenically-influenced Northern Hemisphere midlatitudes. *Geophys. Res. Lett.*, 34: L13801.